University of Kentucky
UKnowledge

Theses and Dissertations--Manufacturing Systems Engineering

Manufacturing Systems Engineering

2019

AN ANALYSIS OF RESISTANCE SPOT WELD QUALITY BASED ON ACOUSTIC AND ELECTRICAL SIGNATURES

Ivan Charles Butler
University of Kentucky, icbutler@icloud.com
Author ORCID Identifier:
https://orcid.org/0000-0001-9260-4503
Digital Object Identifier: https://doi.org/10.13023/etd.2019.252

Right click to open a feedback form in a new tab to let us know how this document benefits you.

Recommended Citation

Butler, Ivan Charles, "AN ANALYSIS OF RESISTANCE SPOT WELD QUALITY BASED ON ACOUSTIC AND ELECTRICAL SIGNATURES" (2019). *Theses and Dissertations--Manufacturing Systems Engineering*. 8.
https://uknowledge.uky.edu/ms_etds/8

This Master's Thesis is brought to you for free and open access by the Manufacturing Systems Engineering at UKnowledge. It has been accepted for inclusion in Theses and Dissertations--Manufacturing Systems Engineering by an authorized administrator of UKnowledge. For more information, please contact UKnowledge@lsv.uky.edu.

STUDENT AGREEMENT:

I represent that my thesis or dissertation and abstract are my original work. Proper attribution has been given to all outside sources. I understand that I am solely responsible for obtaining any needed copyright permissions. I have obtained needed written permission statement(s) from the owner(s) of each third-party copyrighted matter to be included in my work, allowing electronic distribution (if such use is not permitted by the fair use doctrine) which will be submitted to UKnowledge as Additional File.

I hereby grant to The University of Kentucky and its agents the irrevocable, non-exclusive, and royalty-free license to archive and make accessible my work in whole or in part in all forms of media, now or hereafter known. I agree that the document mentioned above may be made available immediately for worldwide access unless an embargo applies.

I retain all other ownership rights to the copyright of my work. I also retain the right to use in future works (such as articles or books) all or part of my work. I understand that I am free to register the copyright to my work.

REVIEW, APPROVAL AND ACCEPTANCE

The document mentioned above has been reviewed and accepted by the student's advisor, on behalf of the advisory committee, and by the Director of Graduate Studies (DGS), on behalf of the program; we verify that this is the final, approved version of the student's thesis including all changes required by the advisory committee. The undersigned agree to abide by the statements above.

Ivan Charles Butler, Student

Dr. Fazleena Badurdeen, Major Professor

Dr. Fazleena Badurdeen, Director of Graduate Studies

AN ANALYSIS OF RESISTANCE SPOT WELD QUALITY BASED ON ACOUSTIC AND ELECTRICAL SIGNATURES

THESIS

A thesis submitted in partial fulfillment of the
requirements for the degree of Master of Science in Manufacturing Systems Engineering
in the
College of Engineering
at the University of Kentucky

By

Ivan Charles Butler

Lexington, Kentucky

Director: Fazleena Badurdeen, Ph.D., Professor of Mechanical Engineering

Lexington, Kentucky

2019

Copyright © Ivan Charles Butler 2019

ABSTRACT OF THESIS

AN ANALYSIS OF RESISTANCE SPOT WELD QUALITY BASED ON ACOUSTIC AND ELECTRICAL SIGNATURES

The union of a set of materials by way of Resistance Spot Welding is designed so that once fused together, a substantial amount of intentional, external force must be applied to separate the contents. Therefore, Resistance Spot Welding is often the preferred fusion method in high-volume manufacturing processes. The result of Resistance Spot Welding however is the formation of a weld nugget which is not visible to the naked eye. Destructive and/or ultrasonic methods applied off-line must be used to determine the quality of each weld; both inefficient and expensive processes. The following research analyzes the data fed back during resistance spot weld sequences in-line and establishes a correlation between emitted characteristics and the final quality of a spot weld.

The two characteristics researched to segregate weld quality are: the electrical sin wave signature and the acoustic sin wave signature produced during the welding sequence. Both features were discovered to have a direct correlation to the final quality of a weld once cured. By measuring and comparing these characteristics at the source, an opportunity is presented to decrease time and potential defects by confirming the quality of each weld in-process and at the source.

KEYWORDS: Acoustic | Electrical Signature | Fast Fourier Transform | Resistance Spot Welding (RSW) | Weld Quality |

Ivan Charles Butler

6/18/2019

Date

AN ANALYSIS OF RESISTANCE SPOT WELD QUALITY BASED ON ACOUSTIC AND ELECTRICAL SIGNATURES

By
Ivan Charles Butler

Dr. Fazleena Badurdeen
Director of Thesis

Dr. Fazleena Badurdeen
Director of Graduate Studies

6/18/2019
Date

DEDICATION

For My Grandmother, Lula.

ACKNOWLEDGMENTS

I would like to extend my sincere appreciation to my Professors, Dr. Dan Seevers, Dr. I.S. Jawahir & Director, Dr. Fazleena Badurdeen for their guidance throughout this process. The department's passion for discovery and willingness to challenge the status-quo served as the inspiration needed to complete this research.

TABLE OF CONTENTS

ACKNOWLEDGMENTS ..... **iii**

TABLE OF CONTENTS ..... **iv**

LIST OF TABLES ..... **vii**

LIST OF FIGURES ..... **viii**

CHAPTER 1. INTRODUCTION **1**

1.1 RESISTANCE SPOT WELDING (RSW) BACKGROUND 1

1.2 RSW LIFE-CYCLE & SUSTAINABILITY 4

1.3 CURRENT RSW QUALITY CONFIRMATION METHODS 5

1.3.1 External Force (Destruct / Chisel Check) 5

1.3.2 Non-Destructive / Ultrasonic Inspection 6

1.4 RESEARCH OBJECTIVE 8

CHAPTER 2. LITERATURE REVIEW **10**

2.1 RESISTANCE SPOT WELDING PARAMETERS 10

2.2 RESISTANCE SPOT WELDING: A HEAT TRANSFER STUDY 13

2.3 ANALYSIS AND DEVELOPMENT OF A REAL-TIME CONTROL METHODOLOGY IN RESISTANCE SPOT WELDING 14

2.4 REAL-TIME INTEGRATED WELD ANALYZER 16

2.5 REVIEW ON TECHNIQUES FOR ON-LINE MONITORING OF RSW PROCESSES 19

2.6 DEVELOPMENT OF AN ONLINE QUALITY CONTROL SYSTEM FOR RESISTANCE SPOT WELDING 24

2.7 SOURCES OF ACOUSTIC EMISSION IN RESISTANCE SPOT WELDING 25

2.8 LITERATURE REVIEW SUMMARY 26

CHAPTER 3. RESEARCH METHODOLOGY 28

3.1 RESEARCH FLOW 28

3.2 EXPERIMENTAL SETUP 29

3.3 EQUIPMENT 30

3.3.1 Spot Welder 30

3.3.2 Oscilloscope 31

3.3.3 Sound Recorder 32

3.3.4 Ultrasonic Inspector 32

3.3.5 Acoustic Software (Audacity) 33

3.3.6 Material Stack-ups 34

3.4 DESIGN OF EXPERIMENTS 35

CHAPTER 4. RESEARCH FINDINGS & COMPARISONS 36

4.1 ACOUSTIC ANALYSIS 36

4.2 ELECTRICAL SIGNATURE ANALYSIS 45

CHAPTER 5. STATISTICAL ANALYSIS SUMMARY 54

CHAPTER 6. CONCLUSION 57

6.1 MACHINE LEARNING & FURTHER RESEARCH 58

APPENDICES 60

[APPENDIX A. PASSING WELD RESULTS] 60

[APPENDIX B. FAILED WELD RESULTS] 70

REFERENCES **80**

VITA **87**

LIST OF TABLES

Table 1-1: Metal Percent Conductivity (Metal Supermarkets, 2015) 2

Table 3-1: Material Thicknesses 35

Table 3-2: DOE Factors 35

Table 4-1: Weld Nugget Diameter Requirement Formulas 36

Table 4-2: Weld 5 DOE Parameters 40

Table 4-3: Weld 5 Ultrasonic Inspection Results 40

Table 4-4: Weld 3 DOE Parameters 42

Table 4-5: Weld 3 Ultrasonic Inspection Results 43

LIST OF FIGURES

Figure 1-1: The RSW Process (Enami, 2016) 3

Figure 1-2: Ultrasonic Inspection C-Scan (Tessonics, 2007) 7

Figure 1-3: Ultrasonic Inspection A-Scan (Tessonics, 2007) 7

Figure 2-1: Finite Element Modeling Analysis for Real-Time Control Methodology (Dia et al., 1991) 15

Figure 2-2: RIWA Transducer Imagery (Tessonics, 2008) 16

Figure 2-3: RIWA Setup Schematic (Tessonics, 2008) 17

Figure 2-4: Dynamic Resistance Curve Welding Different Materials (Ma et al., 2013) .. 20

Figure 2-5: Zr(t) of A Typical Resistance Spot Welding Process (Ma et al., 2013) 21

Figure 2-6: Ideal Electrode Displacement Curve of a Good Weld (Ma et al., 2013) 22

Figure 2-7: Typical Displacement Curve of a Bad Weld (Ma et al., 2013) 22

Figure 3-1: Research Methodology Flowchart 28

Figure 3-2: Research Apparatus Schematic 29

Figure 3-3: Oscilloscope Generated Sin Wave Example 31

Figure 3-4: Audacity Generated Spectrum Graph Example 34

Figure 4-1: Weld 5 Acoustic Divisions 38

Figure 4-2: Weld 5 Acoustic Sin Wave 39

Figure 4-3: Weld 5 Spectrum Frequency Analysis Graph 39

Figure 4-4: Spectrum Frequency Graph Trend: Welds 5, 6, 10, 32 & 34 41

Figure 4-5: Weld 3 Acoustic Sin Wave 42

Figure 4-6: Weld 3 Spectrum Frequency Analysis Graph 42

Figure 4-7: Spectrum Frequency Graph Trend: Welds 3, 9, 13, 25 & 31 44

Figure 4-8: FFT MatLab Script Created (Butler) 46
Figure 4-9: Weld 3 MatLab Generated FFT Plots 47
Figure 4-10: Weld 5 Electrical Sin Wave 48
Figure 4-11: Weld 5 FFT Plot 48
Figure 4-12: Fast Fourier Transform Plot: Welds 5, 6, 10, 32 & 34 49
Figure 4-13: Weld 3 Electrical Sin Wave 50
Figure 4-14: Weld 3 FFT Plot 51
Figure 4-15: Fast Fourier Transform Plot: Welds 3, 9, 13, 25 & 31 52
Figure 5-1: Acoustic Frequency x Pass/Fail 54
Figure 5-2: Electrical Frequency x Pass/Fail 55
Figure 5-3: Acoustic Frequency x Electrical Frequency 56

CHAPTER 1. **INTRODUCTION**

1.1 RESISTANCE SPOT WELDING (RSW) BACKGROUND

Today, the fusion process of welding is widely used and has become a prevalent method of joining sheets of metal together seamlessly. This technique however dates back thousands of years where evidence of soldered joints appears on many artifacts and relics located in Ancient Greece and the Middle East. Throughout the Bronze Age, Iron Age and Middle Ages (~ 3,000 BC to 1,500 AD) welding was a method of creating a diverse set of tools such as hammers, swords, and other weaponry.

Throughout history, the process has derived into several different forms such as Forge Welding, Thermite Welding and more modern techniques such as Arc Welding. The Ashoka Pillar, also known as the Iron Pillar of Delhi located in the QUTB Complex of India is the result of the forge welding process and is a testament to the high caliber of fusion welding possess. Erected near 310 AD, the Iron Pillar has stood the test of time with very little vulnerability to corrosion or joint failures (Al Jader, 2014). Since then, scientific developments throughout the 1800s have led us to one of the most revolutionary derivatives now known as Resistance Spot Welding (RSW). RSW was considered to be first developed by Elihu Thompson throughout the last half of the 19th century during an experiment with copper wires. What gives RSW its niche is the fact it uses the electrical resistance of two metals to generate heat as the basis of the fusion method. A sensitive combination of temperature, pressure and time result in molten metal between the sheets which when cooled becomes the nucleus of the weld known as the weld nugget (Saleem, 2012).

Copper's metallic properties make it an excellent electricity conductor only second to pure Silver allowing 100% of electricity to pass through. Metal Supermarkets (2015) indicates that steel, however, as an alloy of iron, carbon and other elements results in only 3-15% of electrical conductivity in relation to copper. Table 1-1 below illustrates the percent conductivity of various metals in relation to Copper. Copper is used as the industry standard by which electrical materials are rated.

Table 1-1: Metal Percent Conductivity (Metal Supermarkets, 2015)

Ranking	Metal	% Conductivity*
1	Silver (Pure)	105%
2	Copper	100%
3	Gold (Pure)	70%
4	Aluminum	61%
5	Brass	28%
6	Zinc	27%
7	Nickel	22%
8	Iron (Pure)	17%
9	Tin	15%
10	Phosphor Bronze	15%
11	Steel (Stainless included)	3-15%
12	Lead (Pure)	7%
13	Nickel Aluminum Bronze	7%

* Conductivity ratings are expressed as a relative measurement to copper. A 100% rating does not indicate that there is no resistance.

These metallurgical differences result in resistance during the welding process. As the copper electrodes compress the material together at a specific force and electrical current passes through, the resistance of the workpiece against the electrodes generates

heat in between the panels resulting in the molten metal that becomes the weld nugget (Chen et al., 1989). Figure 1-1 below depicts this process. The weld nugget linking two or more sheets of metal is the end product of a RSW process and is what is used to determine the quality of a weld. Analyzing the nugget itself is the only way to determine with complete certainty that the quality of a weld made by means of RSW is good or no good. The analysis of the nugget may be done by either introducing an external force to the weld nugget directly or through ultrasonic inspection. In the automobile manufacturing industry, both procedures are used strategically to ensure each weld on the body of a vehicle meets the necessary design/quality requirements prior to shipping. Resistance Spot Welding is also actively applied in other industries such as battery manufacturing. The production of larger battery assemblies require processes such as Resistance Spot, Ultrasonic or Laser Beam Welding to connect the multitude of battery cells. RSW is often preferred here because of the ability to control temperature in contrast to traditional soldering, which heats and inadvertently decreases the efficiency of the battery (Brand et al., 2015). Other applications include the assembly of small electronic components and even the joining of orthodontic attachments.

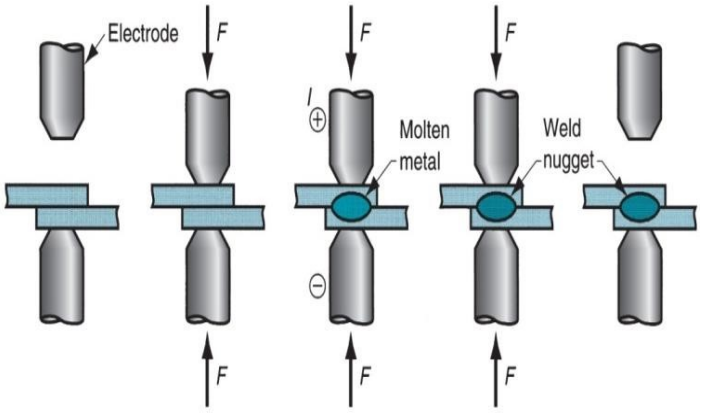

Figure 1-1: The RSW Process (Enami, 2016)

1.2 RSW LIFE-CYCLE & SUSTAINABILITY

The U.S. Government's Bureau of Transportation Statistics (2016) averaged the age of vehicles in operation in the United States at 11.6 years as of 2016. With an increased focus on safety and longevity within the culture of automobile manufacturing, many vehicles are expected to last up to 17 years if properly maintained. Understanding the longevity expected from vehicles speaks to the criticality of a producing a structurally sound product not subject to weld failure. Fatigue of any one of the approximately 5,000 spot welds on a vehicle during its life-cycle has a direct impact on the crashworthiness of a vehicle (Batalha et al., 2012). During pre-production and testing, weld failures will have a negative impact of safety ratings while later in the life-cycle of the vehicle weld failures will directly impact the operator.

Throughout the many industries that Resistance Spot Welding is used in, spot welds are often the subject of cyclic loading. As a result, they are particularly susceptible to failure due to a fatigue fracture (Ertas et al., 2008). This, is due to the relatively small surface area of the fusion points compared to the amount of stress present between the joined sheets. Unlike other welding methods such as mig welding, each weld nugget is isolated from the other rather than one large, fused area between two sheets. This is why design requirements are pivotal in the realm of resistance spot welding regardless of industry or application. In order to reduce the risk of fatigue over time, spot weld joints are designed to reduce stress concentration in a single area and distribute the load as evenly as possible throughout the sub-assembly (Pan et al., 2002). Finite Element Modeling and Simulation Analyses are required to take the inputs of material, design, and weld position to predict the weld's threshold of stress under a given load. Ultimately, the

fatigue of a weld at any point in its life-cycle can result in severe consequences. While there is a certain level of expectation for welds to be designed for optimal performance, there is even more of an onus on the manufacturing end of the spectrum to ensure positive weld quality the first time around.

1.3 CURRENT RSW QUALITY CONFIRMATION METHODS

1.3.1 External Force (Destruct / Chisel Check)

In automobile manufacturing, which is used as the basis of the study, welds confirmed through external force are done traditionally through two methods: Destruct Check & Chisel Check. Remaining ambiguous and not specific to any one automotive manufacturer, prior to any model launch as well as after any significant parameter or material change in a welding process, a destruct test is often required for every weld on the vehicle body. Destruct tests as the name suggests, involve the complete destruction of the spot weld itself to measure its quality. For the Destruct test, AlcoTec (2015) indicates that the tensile strength of the weld nugget is measured by physically peeling the sheets apart until failure. The maximum load required to separate the nugget coupled with the cross-sectional area of penetration determines the overall tensile strength of the weld and whether it meets quality requirements or not.

Chisel Check is also a destructive method of confirming weld quality. The difference with the chisel check method, however, is that the weld is not separated allowing the sub-assembly to continue downstream once confirmed. With the use of a manual or pneumatic chisel and hammer, the chisel is driven in between the two sheets welded together on multiple sides of the weld. With significantly less magnitude than

Destruct check, the sheets are peeled away from each other slightly to determine whether or not the weld nugget will fail. By not failing under the force applied by a standard team member, the quality of the weld is labeled sufficient. Since the weld remains undamaged during this confirmation process, the product can remain in-process and proceed downstream. This characteristic makes chisel check the preferred, daily confirmation method of RSW quality. This method however still requires a significant amount of time and manpower allocated to it. Doing so forces a strategic selection of welds to be chosen for this testing method usually based on their criticality to the end product as opposed to 100% weld confirmation on every vehicle.

1.3.2 Non-Destructive / Ultrasonic Inspection

Within the automobile industry, there is a need for a non-destructive method of weld inspection for product control of the number of vehicle bodies that are scrapped. Beyond Magnetic Particle Inspection & Liquid Penetrant Inspection, both of which are severely meticulous inspection methods, Ultrasonic Inspection (UI) is the most effective non-destructive evaluation method of resistance spot welds. UI avoids any physical threat to the weld's integrity while confirming quality and provides thermal evidence of penetration for any given weld. The probe emits a series of high-frequency sound waves that reflect off of the characteristics of the weld nugget. The strength of the waves as they are emitted and reflected determine the level of penetration present between the two or more sheets of metal. The two outputs of ultrasonic inspection are the C-Scan (Heat Map) & the A-Scan (Reflection Graph). The C-Scan image is a heat map highlighting areas of fusion in the weld. Areas with strong fusion are a deep green as seen in Figure 1-2. Areas with less fusion are depicted with yellow and red indicators. The A-Scan image is a

frequency graph depicting the level of reflection coming off of the back wall of the weld nugget (Figure 1-3).

Figure 1-2: Ultrasonic Inspection C-Scan (Tessonics, 2007)

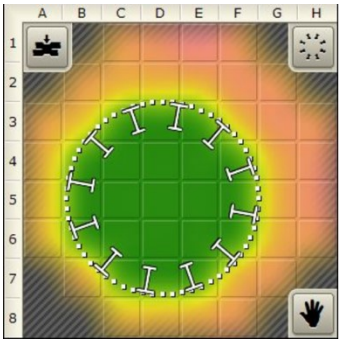

Figure 1-3: Ultrasonic Inspection A-Scan (Tessonics, 2007)

Welds that lack penetration or are “cold” in nature will flat line and not produce any feedback on the A-Scan graph. While this is an extremely effective method in determining the quality of a weld, it is highly inefficient, particularly in a fast-paced, high-volume manufacturing setting. Taking the product/sub-assembly offline, inspecting it ultrasonically and then replacing it in-line would require a significant amount of time and manpower, not conducive to industries where takt times are less than a minute.

1.4 RESEARCH OBJECTIVE

This research seeks to investigate the gaps between the current resistance spot weld quality confirmation methods and their shortcomings with regard to product quality and efficiency.

1) Product Quality: Destructive methods have a direct impact to product quality by either requiring a complete scrap of a sub-assembly post destruct test or by chisel checking only a certain percentage of welds on the vehicle prior to its transfer downstream. This research seeks to eliminate this difficulty by allowing for 100% weld confirmation across each sub-assembly without subjecting welds to any physical stress to determine their quality.
2) Efficiency: While Ultrasonic Inspection is a very accurate method of determining weld quality, it is not feasible to offline vehicles and perform this inspection given the time constraints of high-volume production environments. This research seeks to identify an opportunity of measuring characteristics of the spot weld sequence in-process and at the source eliminating the inefficiency of off lining sub-assemblies to measure them ultrasonically.

The research outlined in the forthcoming sections is organized as follows: Chapter 2 begins with an in depth literature review of all work previously researched in this field and describes how this research seeks to build on those concepts and theories. Chapter 3 will outline the methodology used in conducting this research and experimentation, and detail how the objective will be accomplished. Chapter 4 provides an in depth analysis of the research conducted presenting the raw data obtained from each experiment and how it was analyzed. Chapter 5 summarizes the data statistically in the form of graphical

representations. Chapter 6 ties all aspects of this research together in a conclusion and provides suggestions on how this researched may be furthered.

CHAPTER 2. **LITERATURE REVIEW**

While this concept of classifying weld quality by comparing acoustic and electrical feedback data is unique, the idea of segregating welds based on characteristics in-process is not and has been researched in years prior. To both shed light on, as well as respect the work conducted by those prior, a thorough review of publications in this space was completed, and acknowledgments have been documented respectively. A considerable amount of research was conducted not just on resistance spot welding itself but also the contributing factors to quality, in-process monitoring and life-cycle/sustainability.

2.1 RESISTANCE SPOT WELDING PARAMETERS

As with any other fusion procedure, the output is directly proportional to the series of inputs determined at the beginning of the process. Resistance spot welding is the result of a variety of complex input data that can have a significant impact on the quality of a weld. However, six (6) core parameters have been identified as critical by Rotech Tooling and are listed as follows: *Electrode Force, Electrode Diameter, Squeeze Time, Weld Time, Hold Time & Weld Current* (Robot Welding, 2001).

Electrode Force is the initial compression of the metal sheets together before welding. This parameter is pivotal to overall weld quality as it removes any potential gap between the two sheets allowing a seamless reaction to occur within. In some extremely meticulous applications of Resistance Spot Welding, electrode force varies throughout the process to compensate for the changing electrode diameter and molten material.

Electrode Diameter is directly related to weld nugget size and is therefore crucial in determining the class of weld. A standard rule used across resistance spot welding is that a weld nugget should have a diameter of $(5*t^{1/2})$ (Regalado, 2014). *"t"* in this equation is the thickness of the thinnest sheet of metal being welded. The diameter of the electrode surface must be larger than the required diameter of the weld nugget for a weld to yield any form of positive result.

Squeeze Time is the amount of time in-between the initial application of the electrode force and the first application of current. This parameter secures the workpieces in position until the absolute value of the Electrode Force is attained.

Weld Time is the parameter with the most impact on weld quality. Weld time is the period in which current is passed from the electrodes through the metal sheets. Weld time is a sub-parameter which is adjusted based on a combination of the thickness of the material (nugget size required) and the amount of current passing through. Weld Time is a complex balance of the two because if not dialed in at the correct range can result in either a lack of penetration or an excess of penetration better known as a "blow-out" or "expulsion."

Hold Time, similar to Squeeze Time is the period in which the electrodes are applying force on the materials without current passing through. This parameter, however, occurs after the weld has been made and is in the cooling stage. The force applied while the metal is still somewhat molten allows the nugget to solidify to the desired diameter before being released.

Weld Current, is strictly a measure of the amount of current passing through the electrodes during "Weld Time." Depending on the type of welder this often remains constant.

Throughout the testing period of this research, all six variables were considered during each weld. Electrode Diameter was kept constant throughout the experiment by changing tips frequently once visible distortion of the surface was present. Squeeze and Hold time were also kept constant since a resistance spot welding robot typically regulates them in a production environment. In this instance, a manual spot welder was used to conduct this research. Similarly, Current was kept constant due to the minimal complexity of the welder. Therefore, Electrode Force & Weld Time were the two parameters that were meticulously adjusted when determining the correlation between electrical and acoustic signatures.

2.2 RESISTANCE SPOT WELDING: A HEAT TRANSFER STUDY

The size (diameter) of a weld nugget is directly proportional to the quality of a weld. Welds with smaller nuggets typically lack the penetration required to ensure the sheets of metal will remain fused with little to no chance of separation throughout the life-cycle. Chen et al. (1989) concluded in their white paper that by analyzing the temperature present at the weld source as a function of time, a prediction of the weld nugget size may be made. The correlation between current and time were used here to qualify the quality of a weld. An ideal weld nugget is the result of an optimal balance of current passing through the sheets over time along with a given force applied. The presence of the current generates heat and subsequently a measureable temperature at the fusion point. Chen et al. (1989) generated a theoretical temperature distribution model as a function of time indicating the temperature increase and decrease throughout the weld sequence. By analyzing the temperature over time in comparison to the melting point of the material being joined, this model can indirectly predict the weld nugget size as well the heat affected zone. Consistency across the board is the main concern with this model as inconsistences vary from material to material. Material inconsistencies directly affect how the metals heat and cool as current passes through, subsequently affecting the temperature.

2.3 ANALYSIS AND DEVELOPMENT OF A REAL-TIME CONTROL METHODOLOGY IN RESISTANCE SPOT WELDING

The realm of single parameter in-process monitoring systems has been well studied. Dai et al. (1991) used the Finite Element Analysis method to identify weld quality by comparing the electrode separation occurring in a weld sequence to the thermal expansion and contraction of the weldment. Similarly to above, this relates to the research conducted here in that it uses multiple characteristics of the weld sequence to determine the quality of the weld. Using the Finite Element Method, Dai et al. (1991) developed an expansion-based control algorithm for resistance spot welding. Figure 2-1 below depicts the Finite Element methodology used. Two categories of the weld sequence were distinguished as the mechanical phase and the electrical phase. The finite element program calculates values at each point in the methodology tree ultimately producing two curves. The first curve depicts the range of expansion rate vs the weld time curve. The second curve depicts the range of maximum electrode displacement against the weld time curve. The comparison of the two allows for a prediction regarding the formation of the weld nugget and may be done in-process.

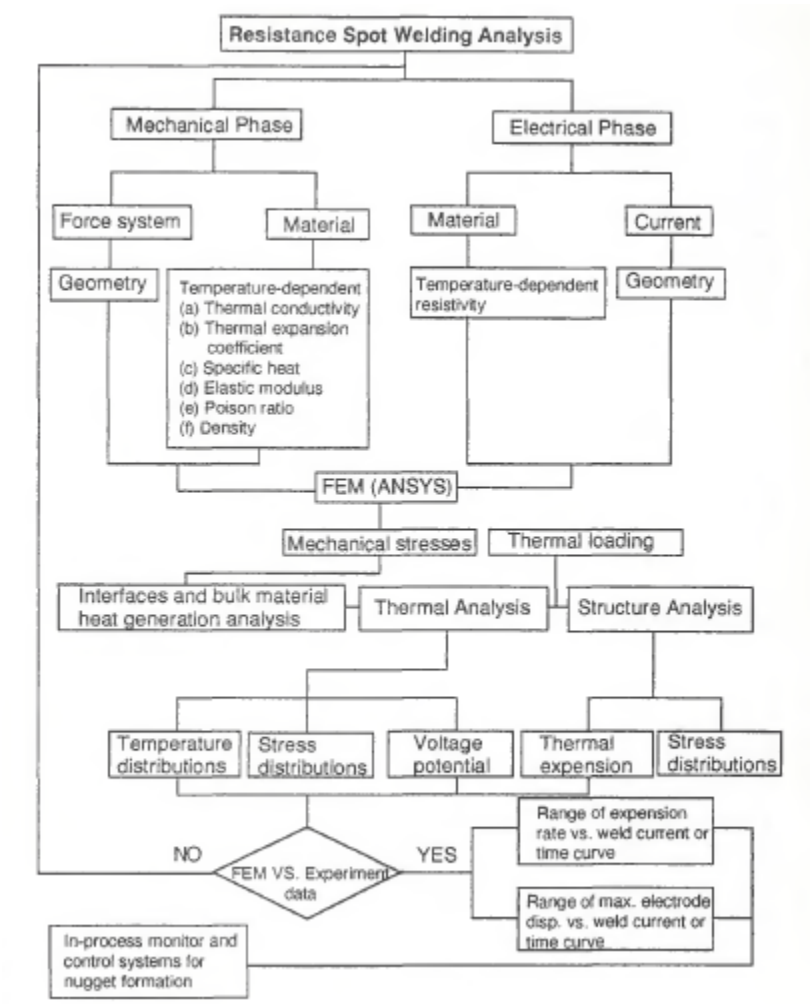

Figure 2-1: Finite Element Modeling Analysis for Real-Time Control Methodology (Dia et al., 1991)

2.4 REAL-TIME INTEGRATED WELD ANALYZER

The work conducted by Regalado (2014) using a non-destructive, real-time monitoring sequence to classify aluminum RSW weld quality closely resembles the objective of this research in identifying the quality of a weld at the source in a production environment. Regalado's research is heavily focused on the use of the Real-Time Integrated Weld Analyzer (RIWA) now marketed by Tessonics Inc., a Canadian start-up focused on Ultrasonic Imaging. The RIWA unit operates through the use of an integrated ultrasonic transducer in one of the copper welding electrodes (Regalado, 2014). Similar to the standard probes used for UI, the transducer sends ultrasonic waves through the upper electrode cap into the sheets of metal being welded which then reflect to the transducer which records them. Figure 2-2 below depicts this process.

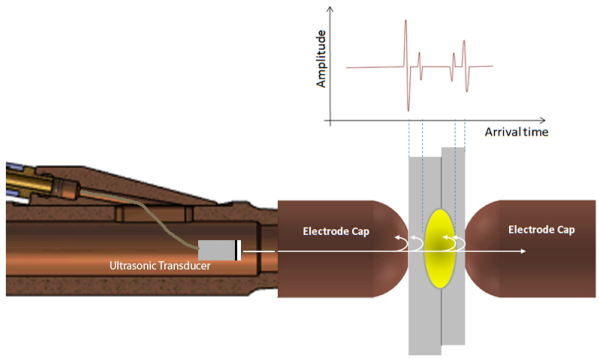

Figure 2-2: RIWA Transducer Imagery (Tessonics, 2008)

The transducer is wired back through the electrode arm of the welder to a PC Quality Monitoring System that analyzes the waves and uses that as a measure of penetration thus allowing it to classify each weld. The PC unit also communicates to the robot controller

passively by extracting weld schedule information for each weld it classifies in a given program shown in Figure 2-3 below.

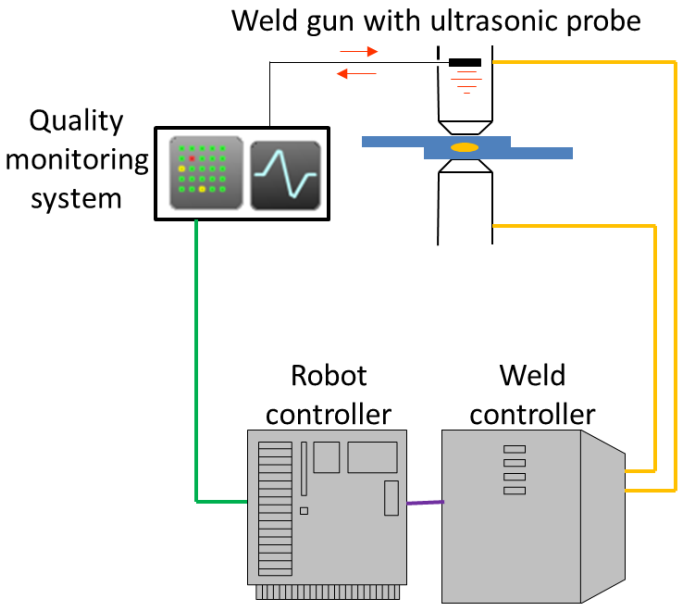

Figure 2-3: RIWA Setup Schematic (Tessonics, 2008)

As previously mentioned, Ultrasonic Inspection is currently the most guaranteed non-destructive method of classifying weld quality. However, the cost associated with such technology is often relatively high compared to its benefit. The RIWA unit, while effective is not conducive to high-volume manufacturing environments that use thousands of robots in the assembly of their final product. Standard Spot-Weld specification robots at a price point of approximately $30,000 can nearly double with the integration of this technology. The research conducted here shares the understanding of a need for in-process monitoring and quality control of resistance spot welds but aims to do so through another method. By classifying the quality of a weld based on its ultrasonic

properties and then comparing both the electrical and acoustic signature generated by each weld, it may be possible to determine at the source whether or not a weld is good based on these characteristics. Furthermore, once this relationship is established, a myriad of samples can be made and used to train a form of Machine Learning algorithm that has the ability to detect the flawed parameter of a bad weld and improve performance for the next cycle.

2.5 REVIEW ON TECHNIQUES FOR ON-LINE MONITORING OF RSW PROCESSES

Preceding the development of the RIWA System, Ma et al. (2013) published a review article on techniques for on-line monitoring of Resistance Spot Welding processes. The group identified the inefficiency of having to off-line products to inspect welds and investigated a series of characteristics present at the source that correlated to the quality of the weld.

The first method investigated was the monitoring of welding parameters related to the power input. Using Dynamic Resistance as an example, this may be used as a calculation of the amount of resistance present at a specific point over a given period of time. Dynamic Resistance is a widely used signal within resistance spot welding that can provide rich information regarding nugget formation (Wang et al., 2016). Throughout the RSW process, dynamic resistance typically yields a three-region curve as depicted in Figure 2-4. Region I represents the immediate drop in resistance due to the breakdown of contact insulation at the beginning of the weld. Region II portraits the increase in dynamic resistance as the workpieces heat up and Region III represents the decrease in resistance as the nugget cools and the process ends. By monitoring deviations in dynamic resistance during the welding process, the team has deemed this a useful method for identifying faults in welding mild-steel. The drawback, however, is the inconsistences dynamic resistance presents from weld to weld depending on characteristics such as thickness and material type.

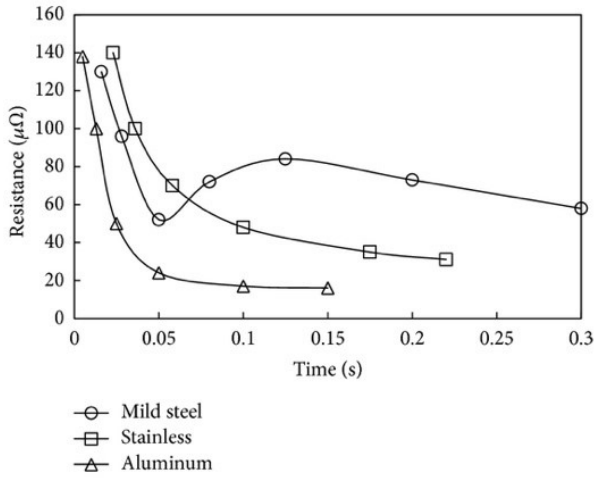

Figure 2-4: Dynamic Resistance Curve Welding Different Materials (Ma et al., 2013)

Input Impedance is another method of monitoring weld parameters related to Power Input studied by this group. Ling et al. (2010) described Resistance Spot Weld systems as electrical circuits consisting of resistance, inductance and capacitance all in series. Once voltage is applied, the response current begins to pass through the circuit. The quotient between these two factors is the resulting input impendence. Figure 2-5 below displays the typical resistance ($Z_r(t)$) in a spot welding process but this time as a function of the electrical impendence, (Z_{in}). It is important to note here that while the difference between a good and bad weld is distinguishable, the patterns are very similar making differentiation on a production level difficult.

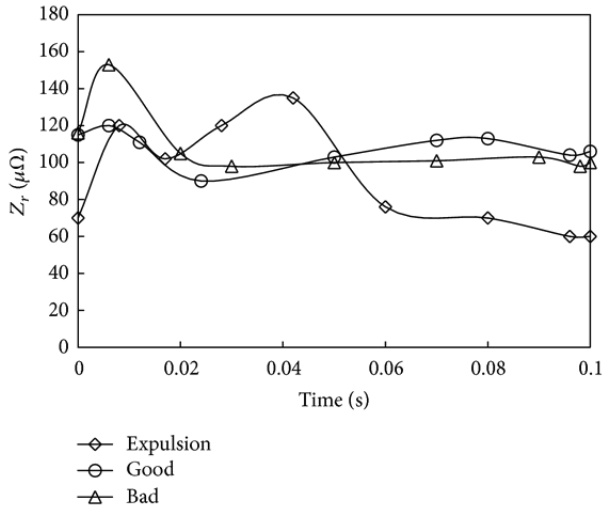

Figure 2-5: Zr(t) of A Typical Resistance Spot Welding Process (Ma et al., 2013)

The second method investigated was monitoring parameters related to mechanical response during the welding process. Both Electrode Force and Electrode Displacement are measurable characteristics during the spot welding sequence. This is closely related to the study of electrode vibration signals during the weld sequence. Although not ideal for industrial, high-volume applications because of the inconvenient installation process of the sensors and high cost, electrode vibrations are still a tangible form of monitoring resistance spot welding quality (Wang et al., 2011). Thermal expansion, melting and expulsion are all aspects that contribute to the behavior of electrode displacement. Figure 2-6 below depicts an ideal displacement curve from a good weld. The pattern represents a very consistent behavior with displacement starting very slowly and then rapidly ramping up as the heat increases and leveling off at the termination of the weld. This representation is contrary to Figure 2-7 which represents a bad weld that blew out depicting a distinguishable difference between the two. The displacement suddenly

spikes downward as there is a loss of contact between the electrode and the sheet of metal.

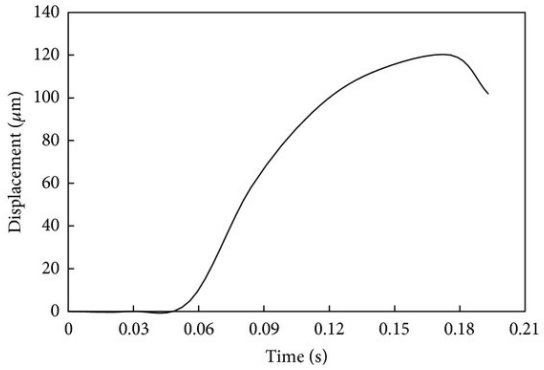

Figure 2-6: Ideal Electrode Displacement Curve of a Good Weld (Ma et al., 2013)

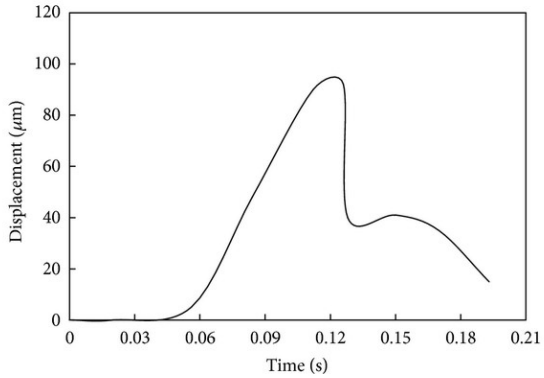

Figure 2-7: Typical Displacement Curve of a Bad Weld (Ma et al., 2013)

Electrode Force was discovered to respond similarly showing visible differences in the graphical representations of good welds and bad welds. The drawback however with both of these measurements is similar to that of the RIWA system. To measure Electrode Displacement accurately, a high-precision laser displacement sensor is required due to the small increments of displacement present proving both inefficient and costly

for a high-volume manufacturing environment. In addition to that, the group also noted that the measurement of the electrode force would require a very complex transducer as the force measurements may easily be manipulated by the electromagnetic forces present during the sequence. The third and final drawback the team identified was the substantial difference in results amongst materials. Force & Displacement measurements as well Dynamic Resistance measurements all vary from mild steel to stainless steel and other metal alloys.

The third mechanical response investigated in their research was acoustic emission. Naturally, when metal is deformed or cracked by force, it emits deformation energy in the form of an elastic wave resulting in an audible sound. Referenced later in this paper is the identification of several different phases of the welding sequence based on the sin wave captured during a resistance spot weld. The challenge identified here was segregation of the welding emissions from the white arbitrary noises present in any manufacturing environment. This difficulty was also faced by Luo et al. (2013) when researching the capability of predicting nugget quality based on structure borne acoustic emission signals. Due to the fact that the microphone is not directly attached to the welding apparatus, the space in-between operates as the transmission medium resulting in additional white noise and potential loss of some acoustic signals. The research conducted for this paper seeks to mitigate that factor by compensating for white and arbitrary noise by not just analyzing the sin wave produced from acoustic emissions but evaluating it as a function of frequency by way of the Fast Fourier Transform algorithm. Doing so allows for a more robust comparison of data when predicting weld quality.

2.6 DEVELOPMENT OF AN ONLINE QUALITY CONTROL SYSTEM FOR RESISTANCE SPOT WELDING

To date, most research analyzing weld quality at the source studies aspects of electrode displacement or electrical parameters such as dynamic resistance. Cho et al. (2000) took it a step further and utilized a neural network to discover a correlation between dynamic resistances and weld nugget quality. The dynamic resistance values were monitored in the primary circuit of the welding machine and then mapped into a vector for pattern recognition. From there the use of the Hopfield neural network classified each of the pattern vectors as functions of weld quality based on nugget size. Similarly, Zhang et al. (2004) utilized a Neuro-fuzzy network system to compare both electrode displacement and electrode velocity during the weld sequence to judge the quality of a weld. Guo et al. (2012) followed suit stating that due to the complexity of the spot welding process and the uncertainty of nugget formation, quality control is a difficult task. Therefore a fuzzy control system comprised of more elements and capturing more data is likely to yield higher control accuracy and quality predictions.

All of the above methods were discussed by Kang (2012) when developing a unique online quality control system for Resistance Spot Welding. The system designed is comprised of two parts: an energy controller and an online nugget diameter estimator. The time spent during the welding cycle is the connection between these two pieces of equipment. A correlation was identified between the input energy of a weld and the nugget diameter by way of a mathematical model. The nugget diameter estimator uses the model to track energy input and angle throughout the weld sequence allowing for the prediction of a weld nugget diameter once the process is complete and the weld has cured. This method addresses the same shortcoming identified in this

research of determining weld quality at the source without physically impacting the weld or removing it from the welding process.

2.7 SOURCES OF ACOUSTIC EMISSION IN RESISTANCE SPOT WELDING

Returning to the realm of audible measurements, there has also been a study conducted on the acoustic emissions of resistance spot welding by Polajnar et al. (2008). In their journal, they analyze the various sound waves produced at select intervals during the welding sequence. By identifying differences in the waves based on the stage of the weld sequence, it was concluded that a limited amount of useful information regarding weld quality might be obtained through the sin wave produced though acoustic emissions. The conclusion they arrived at, however, is that it is **not** possible to distinctly classify weld quality based solely on acoustic characteristics and that additional features must be taken under consideration before classifying a weld.

2.8 LITERATURE REVIEW SUMMARY

This research was conducted within the gap of utilizing two very distinct forms of statistical feedback and measuring them as functions of frequency to determine the quality of a weld. The first contribution made through this research is the instantaneous comparison of two separate data sets of feedback as opposed to a single form of feedback whether electrical or mechanical. As a result, a more reliable method of determining weld quality at the source may be developed. The second contribution made through this research is the introduction of the Fast Fourier Transform algorithm to baseline the data sets captured and allow for a direct comparison as functions of frequency. Previously, weld quality at the source was determined by the measurement of a single characteristic at a time as seen in Polajnar et al. (2008). By introducing the conversion of acoustic signatures as functions of frequency, the white noise is mitigated and more distinguishable from the large peaks that occur in the frequency domains. It also allows for a direct comparison between two data sets that are not naturally comparable.

In reference to the RIWA system researched by Regalado (2014), an incredible opportunity was presented for weld quality to be determined at the source, however, the price point eliminates the feasibility of integration into large scale production operations. This research combats that by studying the quality of a weld based on characteristics that may be captured and interpreted in a more economical way than ultrasonic inspection. Electrical data is currently regulated by the PLC of the robot or spot welder performing the weld sequence and can be captured and measured as a function of frequency. Acoustic emissions may be captured by a standard sound recorder situated within range of the fusion points. The apparatus required to capture both electrical and acoustic

characteristics combined is less expensive than a single ultrasonic probe required for the RIWA unit. This research operates within the gaps of the work mentioned above building on the theories and practices presented ultimately arriving at a more efficient way of determining weld quality in-process.

CHAPTER 3. RESEARCH METHODOLOGY

3.1 RESEARCH FLOW

Figure 3-1 below depicts the flow in which this research was conducted. Beginning with the kitting of raw material and setup of the apparatus, the coupons are then welded together using the resistance spot welder. Three outputs were yielded as the result of a weld sequence: acoustic data, electrical data and weld nugget data. Both the acoustic and electrical data were imported and analyzed through various software channels. The weld nugget data however was analyzed via Ultrasonic Inspection using the Tessonics unit described in section 3.3.4. All three sets of data were then compared against each another and the correlation was documented.

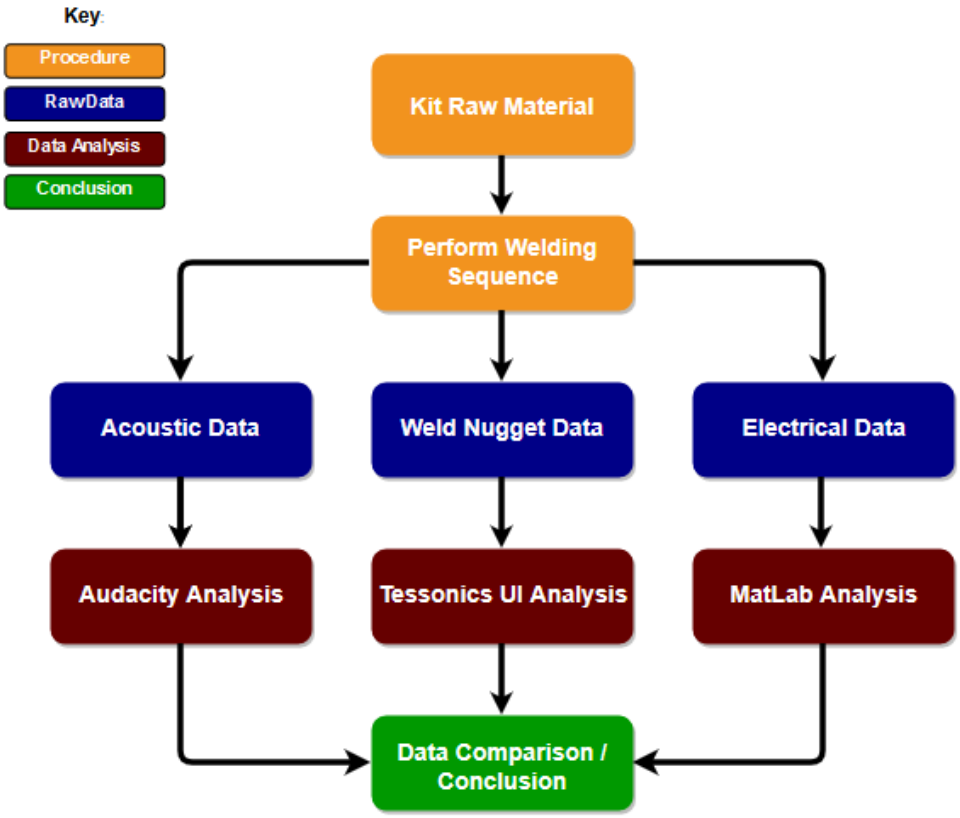

Figure 3-1: Research Methodology Flowchart

3.2 EXPERIMENTAL SETUP

The “Draw IO” schematic in Figure 3-2 below depicts the experimental setup for the research conducted. At the center of the setup is the resistance spot welder with the attached weld timer control, force pedal, and trigger switch. Attached to the bottom electrode is the Oscilloscope cylinder which is wired back to the interface unit. Approximately 100mm away from the weld tips, a Tascam Linear PCM Recorder is set up on a tripod to capture the acoustics during welding. The two sheets of metal being welded are held into place by the operator, myself during the welding cycle. Lastly, sitting away from the welding apparatus is the Tessonics RSWA ultrasonic inspector. Once welding is complete, the coupons are taken over to the RSWA where the weld nugget is analyzed. The RSWA will serve as the baseline control test for this experiment, determining whether welds are classified as “pass” or “fail” based on their penetration

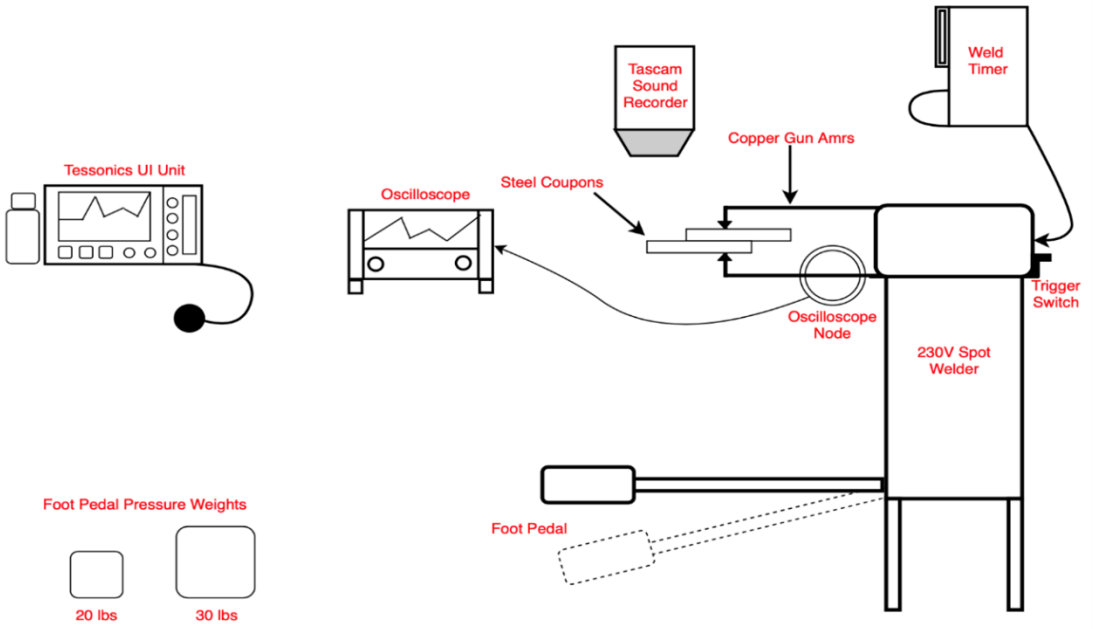

Figure 3-2: Research Apparatus Schematic

3.3 EQUIPMENT

3.3.1 Spot Welder

The spot welder used for this research is a 230V electrically timed Miller spot welder. The welder consists of two copper electrodes each with Miller OEM weld tips aligned perpendicularly at the end. Weld time is controlled exclusively by the Miller weld timer connected to the body of the welder. Weld Time, as one of the core parameters outlined above related to weld quality, was adjusted between 0.5 and 1 second(s) throughout the experiment. During initial trials of the research, it became apparent that for the material thickness being studied, a weld sequence with weld time longer than 1 second would typically result in a blowout weld due to the excess amount of current. Contrarily, any weld with a weld time held under 0.5 seconds would result in an insufficient nugget generated to bond the steel coupons together. The foot pedal of the welder controls Electrode Force. To maintain a level of consistency throughout testing and not leave the parameter susceptible to human error, metal weights of 20lbs and 30lbs (88.96N & 133.45N) classified as light, and heavy pressure respectively were used. Once the coupons are positioned between the electrode and the force has been applied via the foot pedal, myself the operator pulls the “trigger” switch behind the welder that releases the current through the electrodes for the time designated by the weld timer, and the materials are bonded together.

3.3.2 Oscilloscope

The oscilloscope used throughout the testing phase was a Textronix MSO/DPO3000 Mixed Signal Oscilloscope. A HARTING Hall Effect Sensor (HCM 200A) was placed over the lower electrode of the Miller welder and wired directly to the oscilloscope. During each weld sequence, the oscilloscope was tuned to capture ~ 10,000 data points over a two second period. Each weld resulted in a sin wave varying in amplitude representing the different voltages present in the electrode during the weld. Figure 3-3 below represents the output of the oscilloscope after one weld. In addition to displaying just the graph, all data points are captured and exported in a .csv file from the oscilloscope. The .csv file was uploaded to Microsoft Excel displaying the data points and graphed once again. Once exported to excel, the data was also stored and imported to MatLab to plot the sin wave as a function of Frequency using the **Fast Fourier Transform** algorithm (FFT). FFT was used to plot both the acoustic emissions and electrical signatures as functions of frequency against time.

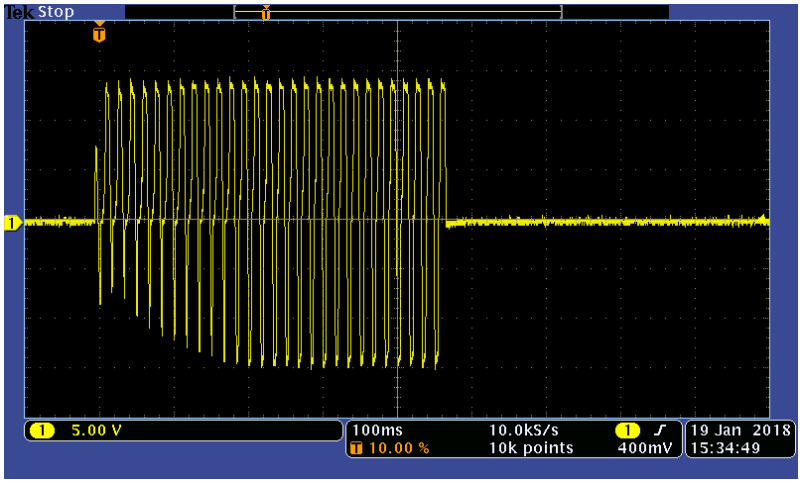

Figure 3-3: Oscilloscope Generated Sin Wave Example

3.3.3 Sound Recorder

The audio recorder used to capture the sound of each weld was a Tascam DR-40 Handheld 4-Channel Recorder. As a relatively "high-end" recorder, the DR-40 was ideal for capturing the relatively small audio distortions present during the welding sequence. The experiment was conducted in Lexmark's research and machine shop with an average white noise range of 60-65 dB. The Tascam recorder did an excellent job in segregating the "white noise" from the welding acoustics. This can be seen through the sonic signature analysis done using Audacity. During the research period, the Tascam sound recorder was set up on a tripod 100mm away from the contact point of the two electrodes. Prior to each weld being conducted, myself the operator, would call out the material stack up, the force being applied and when the trigger was about to be pulled for the weld sequence to begin. Doing so allowed for a more distinct indication of when the weld began and ended.

3.3.4 Ultrasonic Inspector

The baseline control test for this experiment was a Tessonics Resistance Spot Weld Analyzer (RSWA) F1. The ultrasonic inspection device is used to measure the penetration of a range of spot welds and produce thermal images of their contents on a screen. More specifically, this device is tailored to two-sheet and three-sheet welds with plate thicknesses ranging from 0.5mm to 2.4mm. Mild steel, high strength steel, and dual phase ultra-high strength steel with bare, zinc and e-coatings are all potential stack-ups the ultrasonic inspector can read. The UI unit was used to confirm the weld quality of each weld made during the experiment confirming the theory of whether or not a weld was "good" or "bad" based on acoustic and electrical signature comparisons. This

baseline will prove useful in the machine learning aspect of the research to assist with training samples.

3.3.5 Acoustic Software (Audacity)

Each audio file captured by the Tascam sound recorder was imported and analyzed using the open-source digital audio editing software, Audacity. Audacity was chosen mainly because of its interactive user interface and ability to critically analyze a high volume of data points. Once the audio file (.wav) is imported to Audacity, a sin wave is displayed showing the length of the file. The vertical y-axis on the left-hand side of the screen ranges from -60dB to 0dB in which 0 is the threshold for sound recording as it often becomes distorted beyond that point. The horizontal x-axis plots time of the weld which is regulated by the weld timer. When analyzing the acoustic wave, it is evident that the length of the sound wave generated from the weld sequence is equal to the length of time set on the weld timer. With this information, the weld sequence time was extracted from the overall .wav file, and a spectrum diagram was plot. The spectrum diagram plots the sound sample against its component frequencies (Figure 3-4). This is done once again using the mathematical algorithm known as Fast Fourier Transform. FFT takes the sum of all sinusoidal waves captured during the weld sequence and identifies the variable frequencies. Doing so allows us to identify the peak frequencies in each weld sequence. Anticipating that there is a difference in peak frequency between what is classified as a good weld and what may be classified as a bad weld, this information was captured for each weld sample and plotted. Results are discussed in the comparison section below.

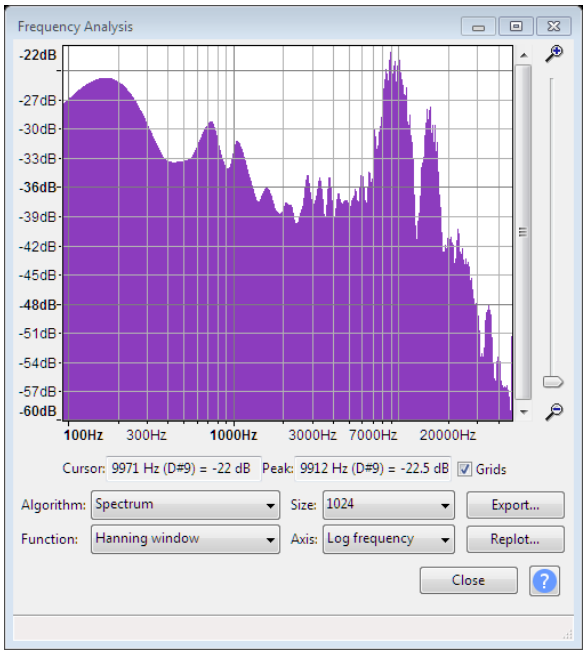

Figure 3-4: Audacity Generated Spectrum Graph Example

3.3.6 Material Stack-ups

To best relate to high volume manufacturing processes, the material used to conduct this research was industrial grade cold rolled Galvannealed (CR Base) steel with a minimum tensile strength of 39.2 ksi. (SCGA270D). Two separate thicknesses (1 mm / 0.5 mm) were chosen to investigate whether or not acoustic and electrical signatures varied based on the thickness of the material being welded together. The steel was cut into sample coupons 150mm x 200mm in dimension. All steel of each thickness was procured from the same blank to reduce inconsistencies in the metal. Therefore, each coupon was rolled, treated and cut in the same way as the other. The material was classified as described below in Table 3-1.

Table 3-1: Material Thicknesses

Material	Thickness (mm)
A	1.0
B	0.5

Each variation of material was welded together with a total of six welds. Three welds were made using the 20lb pressure plate, and three were made using the 30lb pressure plate. All six welds on each of the coupon variations were measured using the Tessonics Ultrasonic Inspection unit to determine the amount of penetration present and classify each as either a good or bad weld.

3.4 DESIGN OF EXPERIMENTS

To effectively control the research conducted, a design of experiments (DOE) was implemented. Doing so has allowed us to understand which parameters have a significant impact on the process output and which output is affected by different parameter levels. Outlined in Table 3-2 below is the Two-level Factorial Design parameters and the levels of each. The output response for each variation will be the quality of each weld which is measured by the Tessonics Ultrasonic Inspection unit and classified as “pass” or “fail.”

Table 3-2: DOE Factors

Factor	Name	Units	Low Level (-)	High Level (+)
A	Weld Time	Seconds (s)	0.5	0.75
B	Electrode Pressure	Pounds (lbs)	20	30
C	Material	Millimeters (mm)	0.5	1.0

CHAPTER 4. **RESEARCH FINDINGS & COMPARISONS**

4.1 ACOUSTIC ANALYSIS

To identify a trend between both acoustic and electrical signatures, the two signals must be measured against the same baseline to provide an accurate result. Over 500 welds were analyzed during this research period. A sub-set of five (5) passing and five (5) failing welds will be discussed throughout this research to outline the discoveries made in more detail. This subset represents the average trend of behavior for both acoustic and electrical data. The baseline control test results from the Ultrasonic Inspector are captured in a table below each weld sequence, classifying the weld. Weld classes are defined as "A Class," "B Class," & "C Class." The classes are determined through the formulas presented in Table 4-1 below:

Table 4-1: Weld Nugget Diameter Requirement Formulas

Weld Class	Formula
A Class Weld	$\sqrt{(Thinnest\ Sheet)} \times 5$
B Class Weld	$\sqrt{(Thinnest\ Sheet)} \times 4$
C Class Weld	$\sqrt{(Thinnest\ Sheet)} \times 3$

This formula is used as a rule of thumb in many high-volume weld manufacturing processes. In order for a weld to pass it must classify as an A or B class weld meaning the diameter of the nugget produced must be equal to or larger than the square root of the thinnest sheet being weld together multiplied by a constant of 5 for "A Class" and a constant of 4 for "B Class". Weld nuggets that are smaller than four times the square root of the thinnest sheet are deemed "C Class" welds and do not pass quality inspection. The

diameter of the nugget is a direct output of the Tessonics UI unit along with the C-Scan heat map.

Polajnar et al. (2008) in their publication previously identified six different divisions of the acoustic wave produced in a spot weld. They are defined as the following:

1) Free-Laying / Ambient Noise: This is the surrounding white noise of the shop being picked up by the sound recorder prior to the work pieces being welded.
2) Electrode Approach & Pre-Pressure: This constitutes to the noise generated from the initial contact of the electrode to the workpieces and pressure is applied.
3) Welding: This is the most extended segment of the acoustic wave which is comprised of the period in which electrical current is being passed through the electrodes and the workpieces slowly become molten. This is often the most uniform section of the wave.
4) Nugget-forging: This occurs in the instance immediately after the current has stopped being applied and the electrodes are still applying pressure. During this period, the molten metal begins to form into the weld nugget expected.
5) Electrode Release: Once the electrical current ceases and the hold time has subsided, the electrode force is released, and the tips are removed from the workpieces. This action generates a small distortion in the acoustic wave that is picked up by the sound recorder.
6) Free-Laying/Cooling Phase: This segment occurs post electrode release while the workpiece is cooling down and the weld nugget is completing its cure. This phase is not very distinctive and is often hard to separate from white noise on the back end of the weld.

Using Weld 5 as an example, we can see in Figure 4-1 below that these characteristics hold true in not just this one, but all welds conducted. While they are not all identical, they all follow this primary sequence that can be identified by isolating specific time sequence of the weld.

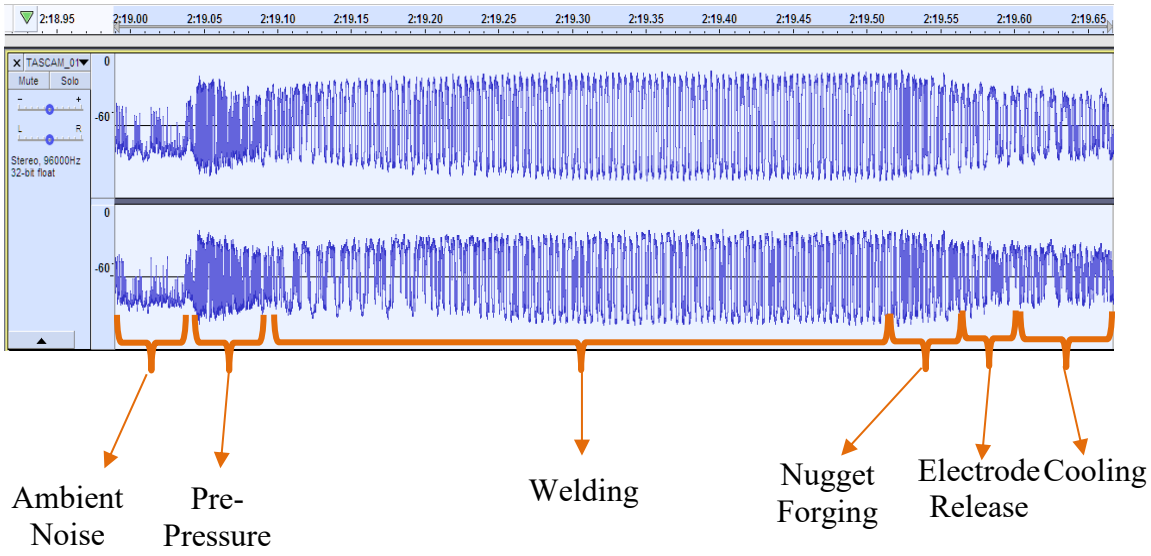

Figure 4-1: Weld 5 Acoustic Divisions

The detailed data for Weld 5 presented below serves as an example representing the average consensus of all weld results that yielded a "good" or passing result based on the ultrasonic inspection. Data for the four other welds detailed in this research and classified as passing may be found in Appendix A. Beginning with the analysis of the acoustic sin wave produced, it is evident that they all resemble each other at different points throughout the welding sequence. Figure 4-2 depicts the raw acoustic wave captured by the Tascam sound recorder and imported into Audacity. Figure 4-3 shows the spectrum frequency analysis graph generated from the same weld sequence. Table 4-2

details the parameters used in relation to our design of experiments while Table 4-3 details the results of the weld quality baseline control yielded by the Tessonics Ultrasonic Inspection Unit.

Acoustic Analysis of a Passing Weld Performance: Weld #5

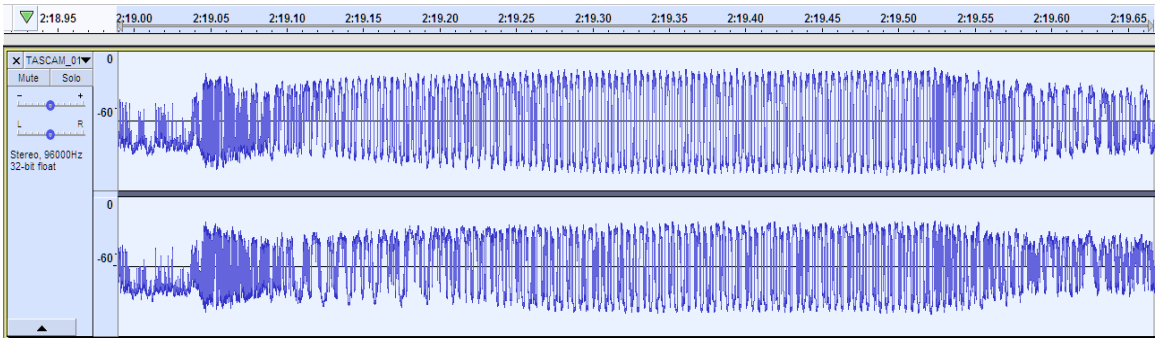

Figure 4-2: Weld 5 Acoustic Sin Wave

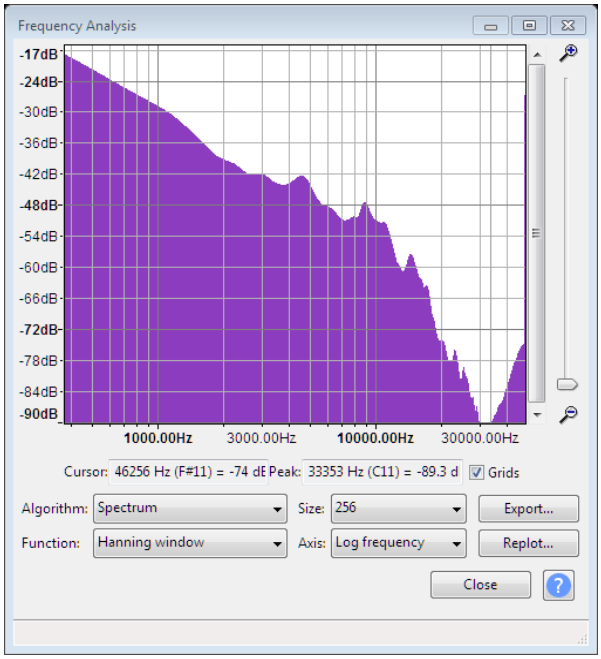

Figure 4-3: Weld 5 Spectrum Frequency Analysis Graph

Table 4-2: Weld 5 DOE Parameters

Material	Pressure	Weld Time
A x A (1.0mm)	Heavy (30 lbs)	0.5 seconds.

Table 4-3: Weld 5 Ultrasonic Inspection Results

Decision		Weld	Diameter		Classification	C-Scan
Pass/Fail	Reason	ID	Required (A-Class)	Measured	A,B,C, Cold	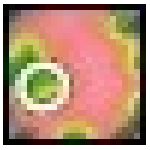
Pass	-	Weld005	5	4.0	B Class	

The trend captured here in the spectrum frequency analysis graph of each weld is what defines the difference between welds classified by the UI as good or bad. The spectrum frequency analysis graph for Weld 5 in comparison to the four others detailed in this research and classified as passing is shown in Figure 4-4 below. As a function of frequency, it becomes evident that this linear down trend, indicated by the orange dashed line is present in each weld sequence. These welds classified as "good" or of a passing grade all possess uniform frequency graphs with peak frequencies ranging from 1,000-4,000 Hz.

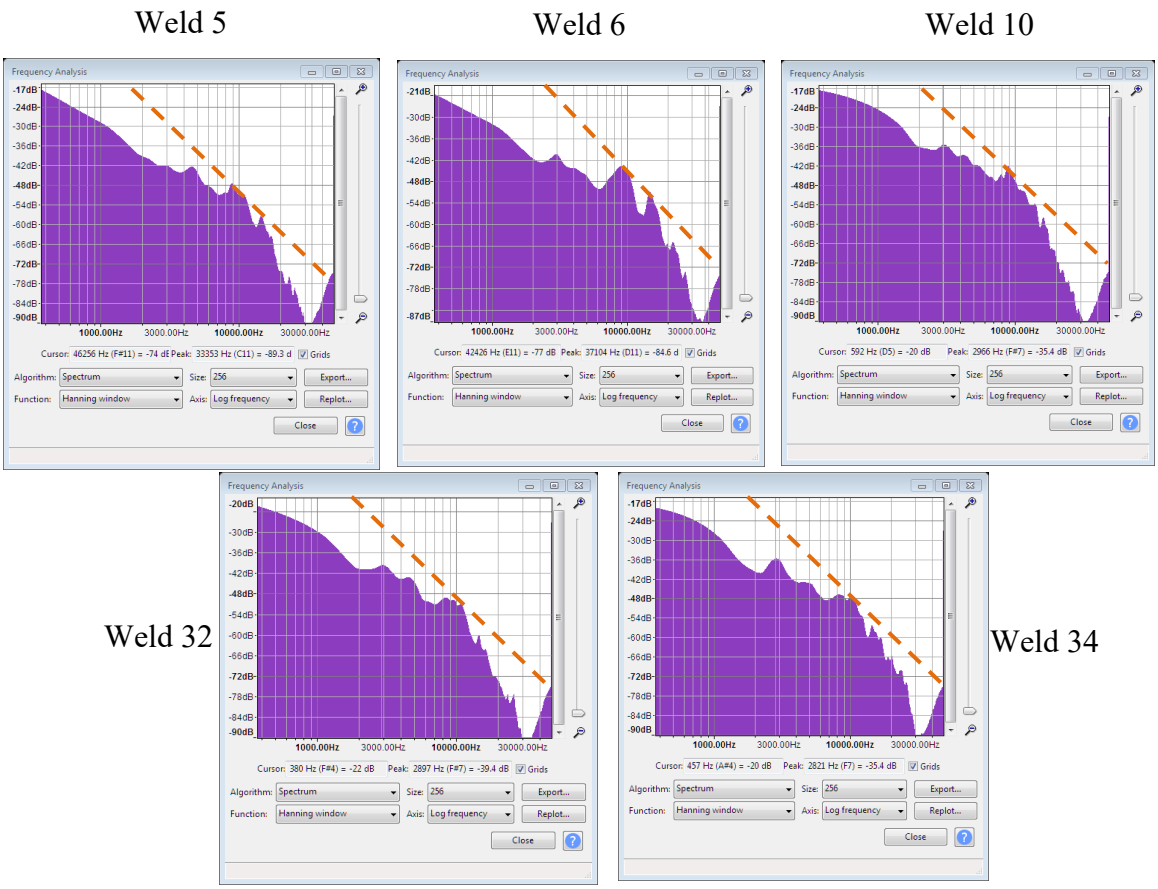

Figure 4-4: Spectrum Frequency Graph Trend: Welds 5, 6, 10, 32 & 34

Acoustic Analysis of a Failing Weld Performance: Weld #3

To compare trends, the data for Weld 3, a weld classified as a failed weld is presented below as a representation of the common trend identified in welds that failed inspection. The four other failing welds detailed in this research are located in Appendix B. Similar to before, Figure 4-5 depicts the raw acoustic wave captured by the Tascam sound recorder and imported into Audacity. Figure 4-6 shows the spectrum frequency analysis graph generated from the same weld sequence. Table 4-4 details the parameters used in relation to our design of experiments while Table 4-5 details the results of the weld quality baseline control yielded by the Tessonics Ultrasonic Inspection Unit.

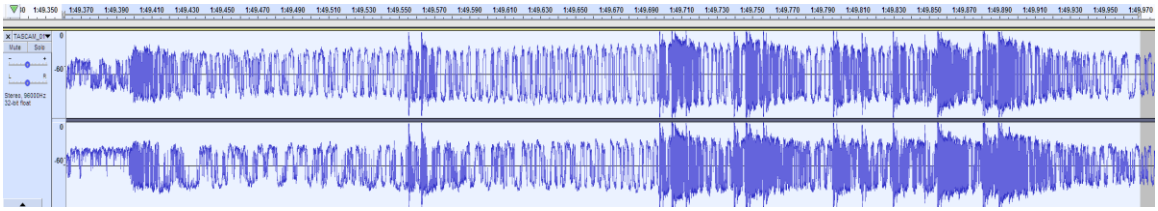

Figure 4-5: Weld 3 Acoustic Sin Wave

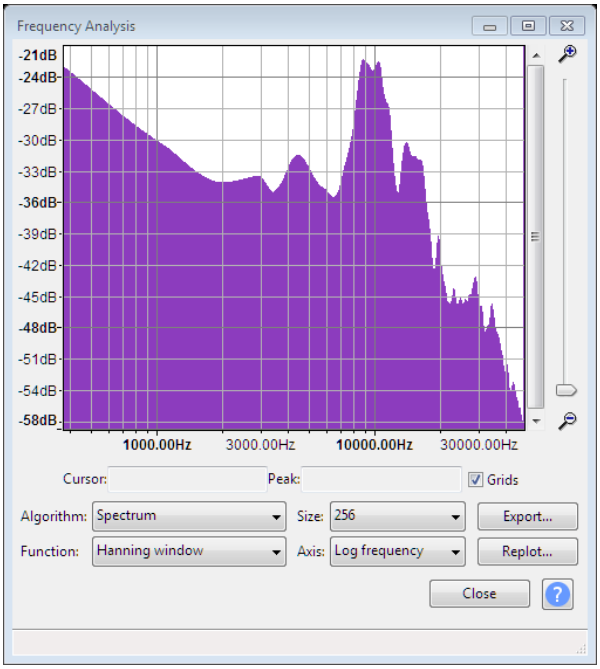

Figure 4-6: Weld 3 Spectrum Frequency Analysis Graph

Table 4-4: Weld 3 DOE Parameters

Material	Pressure	Weld Time
A x A (1.0mm)	Light (20 lbs)	0.5 seconds.

Table 4-5: Weld 3 Ultrasonic Inspection Results

Decision		Weld	Diameter		Classification	C-Scan
Pass/Fail	Reason	ID	Required (A-Class)	Measured	A,B,C, Cold	
Fail	RSWA Cold	Weld003	5	N/A	Cold	

The data for weld three shown above in addition to all other no good welds presented in Appendix B possess a unique acoustic trend. Contrary to the frequency analysis graphs of the welds classified as good, these welds do not follow a linear trend but instead have a significant spike later in the sequence. The peak frequency for these welds lands between 10,000 and 20,000 Hz. What this indicates is that throughout the weld sequence for each weld classified as no good there is some abnormal sound of significant volume occurring which produces a higher frequency point. Failed welds occurring here were labeled as failures for one of the following reasons: Undersized Nugget, No Nugget (Cold Weld), or Visual Pinhole (Blowout). The first two reasons are directly related to the amount of pressure applied between the electrode tips and the metal coupons themselves. If not perfectly flush with the tips at 90-degree perpendicular angles, a gap is created in the weld stack-up. Gaps in the weld stack-up allow for what we consider "Spatter" which is the escape of microparticles of the molten metal from the reaction in the form of sparks (Al Jader et al., 2010). The formation of this spatter is a contributor to the abnormal acoustic emission during the weld sequence thus producing the spike in peak frequencies. The third classification mentioned above is a pinhole or blowout in the weld which is strictly an excess of molten metal between the two sheets resulting in a physical hole where the weld nugget is expected to be. The spike in acoustic frequency here is a result of not just spatter escaping from the tips but now a

lack of material being present between the electrodes while they continue to exert a high level of current. The abnormal acoustic signature of Weld 3 in Figure 4-5 shows the point during the sequence in which the material had diminished resulting in an erratic sin wave.

From the acoustic data studied on both good and bad welds, we may note that there is a distinctive difference between the two when analyzed as functions of frequency. Passing welds that yield a sufficient nugget between the two materials result in peak frequencies within the range of 1,000-4,000Hz. Failed welds resulting in little to no nugget at all generated between the sheets yields peak frequencies much higher within the realm of 10,000-20,000Hz indicated by the orange dashed circle in Figure 4-7 below.

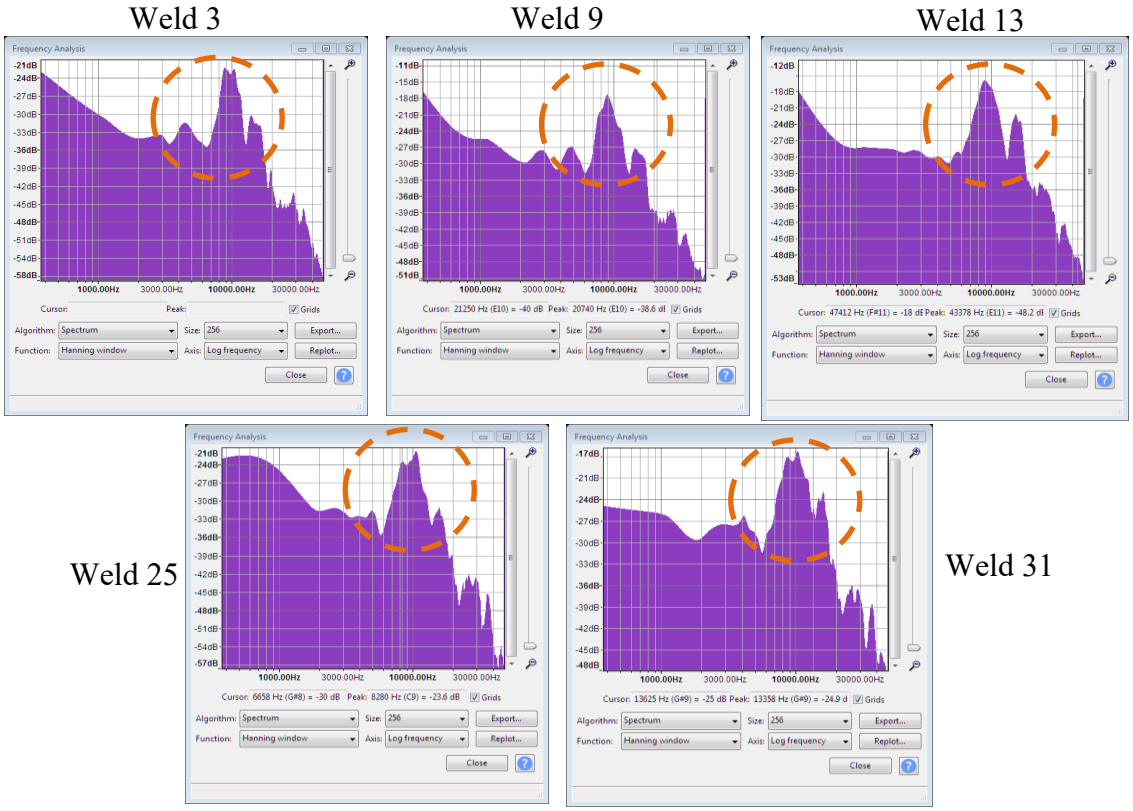

Figure 4-7: Spectrum Frequency Graph Trend: Welds 3, 9, 13, 25 & 31

4.2 ELECTRICAL SIGNATURE ANALYSIS

Similar to the acoustic analysis presented, the electrical signature of the same ten welds (five good / five bad) are analyzed to discover a distinction between welds classified as good and bad. The tabled results dictating DOE Parameters as well as Ultrasonic Inspection Results will remain the same. The first figure presented for each weld will be the sin wave generated using the 10,018 data points captured from the Harting Hall Effect Sensor. The Sin Wave was initially generated by the oscilloscope and then plotted again using Microsoft Excel & MatLab to confirm accuracy. The second figure presented for each weld will be the Fast Fourier Transform Analysis Graph generated using MatLab. The '.m' script displayed below in Figure 4-8 was written to extract the 10,018 data points of each weld stored in multiple sheets of a single Microsoft Excel file. Once the data points are extracted, the code directs MatLab to perform a Fast Fourier Transform (FFT) Analysis on the combination of points. The script then prompts a plot of the absolute value of these data points producing a graph depicting the electrical signature as a function of magnitude against frequency bins. The graph produced shows a mirror image of the peak frequencies produced during that weld sequence indicating that only one side of the spectrum effectively needs to be analyzed.

Butler_ThesisResearch_EAScript.m

```
%Butler - Thesis Research - Electrical Analysis Script
%Fs = 10kHz
%Bad Weld 1 = Weld 3
BOne = xlsread('Butler_ThesisResearch Round 2.xlsx','AxA Weld 3','A19:B10018')
BOneFFT = abs(fft(BOne))
figure('Name','Failed Weld 1: FFT Analysis','NumberTitle','off')
plot(BOneFFT)
%Bad Weld 2 = Weld 9
BTwo = xlsread('Butler_ThesisResearch Round 2.xlsx','BxB Weld 3(9)','A19:B10018')
BTwoFFT = abs(fft(BTwo))
figure('Name','Failed Weld 2: FFT Analysis','NumberTitle','off')
plot(BTwoFFT)
%Bad Weld 3 = Weld 13
BThree = xlsread('Butler_ThesisResearch Round 2.xlsx','BXB Weld 7(13)','A19:B10018')
BThreeFFT = abs(fft(BThree))
figure('Name','Failed Weld 3: FFT Analysis','NumberTitle','off')
plot(BThreeFFT)
%Bad Weld 4 = Weld 25
BFour = xlsread('Butler_ThesisResearch Round 2.xlsx','AxA W1(25)','A19:B10018')
BFourFFT = abs(fft(BFour))
figure('Name','Failed Weld 4: FFT Analysis','NumberTitle','off')
plot(BFourFFT)
%Bad Weld 5 = Weld 31
BFive = xlsread('Butler_ThesisResearch Round 2.xlsx','BXB W2(31)','A19:B10018')
BFiveFFT = abs(fft(BFive))
figure('Name','Failed Weld 5: FFT Analysis','NumberTitle','off')
plot(BFiveFFT)
%Good Weld 1 = Weld 5
GOne = xlsread('Butler_ThesisResearch Round 2.xlsx','AxA Weld 5','A19:B10018')
GOneFFT = abs(fft(GOne))
figure('Name','Passed Weld 1: FFT Analysis','NumberTitle','off')
plot(GOneFFT)
%Good Weld 2 = Weld 6
GTwo = xlsread('Butler_ThesisResearch Round 2.xlsx','AxA Weld 6','A19:B10018')
GTwoFFT = abs(fft(GTwo))
figure('Name','Passed Weld 2: FFT Analysis','NumberTitle','off')
plot(GTwoFFT)
%Good Weld 3 = Weld 10
GThree = xlsread('Butler_ThesisResearch Round 2.xlsx','BxB Weld 4(10)','A19:B10018')
GThreeFFT = abs(fft(GThree))
figure('Name','Passed Weld 3: FFT Analysis','NumberTitle','off')
plot(GThreeFFT)
%Good Weld 4 = Weld 32
GFour = xlsread('Butler_ThesisResearch Round 2.xlsx','BxB W3(32)','A19:B10018')
GFourFFT = abs(fft(GFour))
figure('Name','Passed Weld 4: FFT Analysis','NumberTitle','off')
plot(GFourFFT)
%Good Weld 5 = Weld 32
GFive = xlsread('Butler_ThesisResearch Round 2.xlsx','BxB W5(34)','A19:B10018')
GFiveFFT = abs(fft(GFive))
figure('Name','Passed Weld 5: FFT Analysis','NumberTitle','off')
plot(GFiveFFT)
```

Figure 4-8: FFT MatLab Script Created (Butler)

Using Weld 3 as an example, presented below in Figure 4-9 are three images of the FFT Analysis. The first image in the top left is of the entire graph showing the mirrored results of the 10,018 data points. The second image in the top right illustrates the focus on the single left-hand side of the spectrum. The final image at the bottom which is the image that will be displayed in the results below is the higher resolution image of the FFT highlighting where the peak frequencies lay.

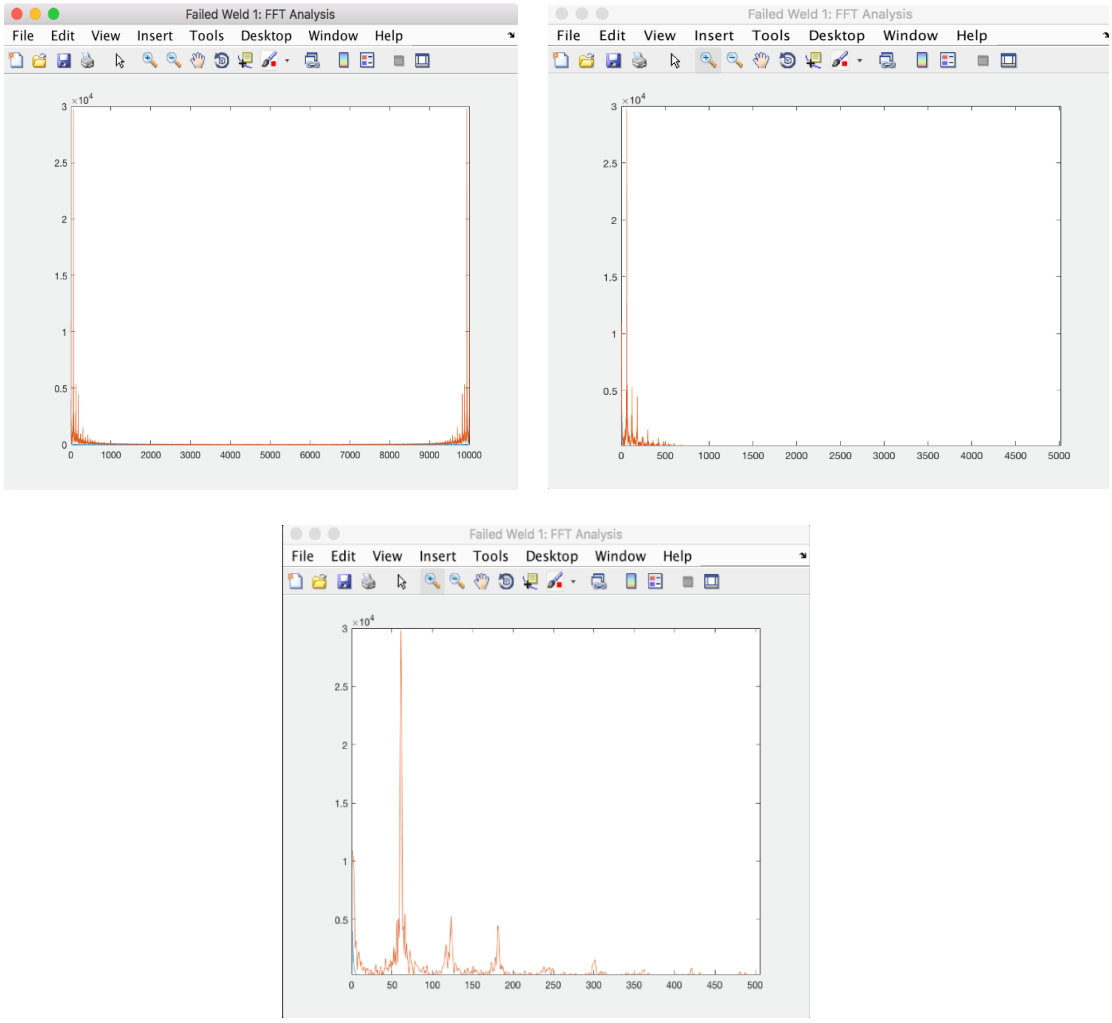

Figure 4-9: Weld 3 MatLab Generated FFT Plots

Electrical Signature Analysis of a Passing Performance: Weld #5

Presented below is Weld 5 analyzed electrically in a similar way that it was acoustically in the previous section. Similar to before, the data for Weld 5 will serve as a representation for all other passing welds referenced in Appendix A. Figure 4-10 below represents the raw electrical signature captured by the Textronix Oscilloscope and plot as a function of voltage over time. Figure 4-11 depicts the same data points captured in

Figure 4-10 but plot as a function of frequency using the Fast Fourier Transform Algorithm. For the DOE parameters used during this weld sequence, reference Table 4-2. For results yielded by the Tessonics Ultrasonic Inspection unit, reference Table 4-3.

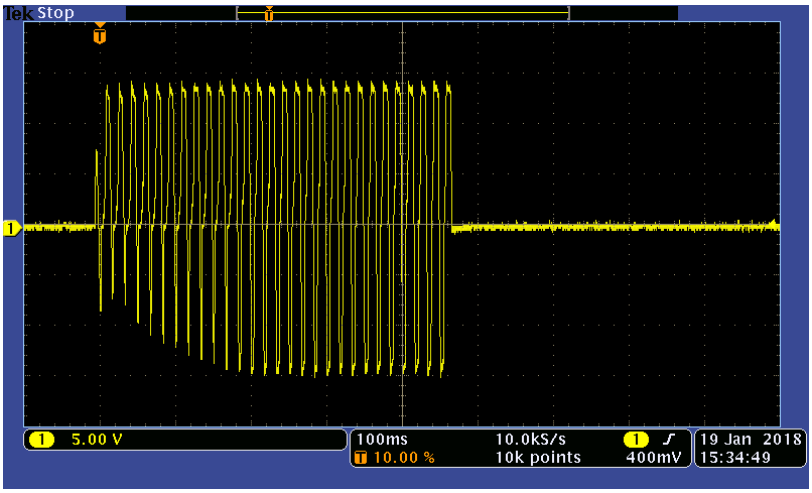

Figure 4-10: Weld 5 Electrical Sin Wave

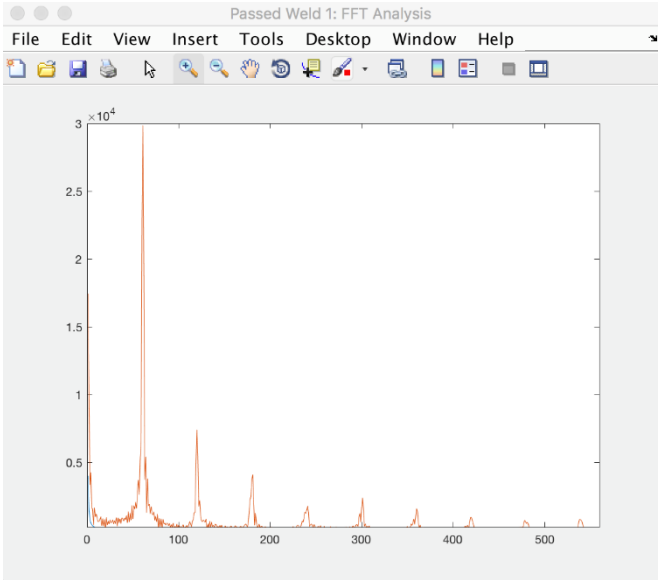

Figure 4-11: Weld 5 FFT Plot

The data above for weld 5 indicates that four distinct peak frequencies were generated from the weld. The x-axis of the FFT graph dictates frequency in bins which

must be converted to Hz to have a direct comparison to the acoustic frequency. The 10,018 data points were all captured over a time domain of two seconds yielding a sampling frequency of 5,009 samples per second. Effectively analyzing just one half of the mirrored graph, our x-axis may be converted from frequency bins to frequency in Hz by dividing the sampling frequency in half. Therefore, the displayed range of each weld with an x-axis of 0-500 frequency bins represents 0-250Hz. Weld 5 and all other welds classified as passing, yield four notable frequencies at 0.5Hz, 31Hz, 62Hz & 91Hz as indicated by the blue dashed circles in Figure 4-12 below. It should also be noted that while the magnitude of each peak varies based on the weld sequence, our focus is on the frequency point at which the peak occurs.

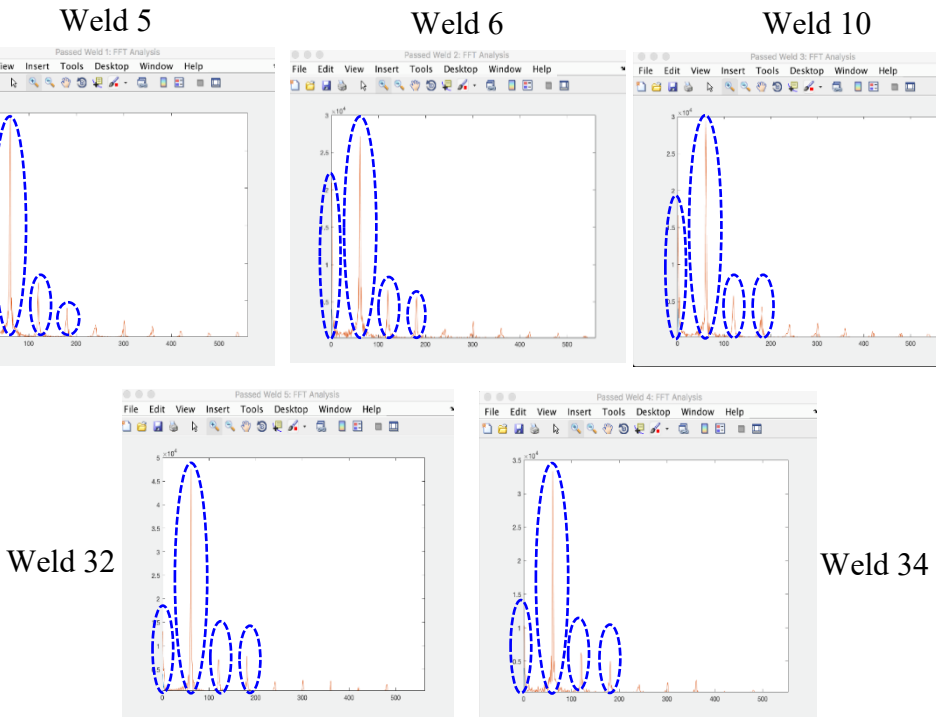

Figure 4-12: Fast Fourier Transform Plot: Welds 5, 6, 10, 32 & 34

To compare trends, the electrical data for Weld 3, a weld classified as a failed weld is presented below as a representation of the common trend identified in welds that failed inspection. All other failing welds are located in Appendix A. Figure 4-13 below represents the raw electrical signature captured by the Textronix Oscilloscope and plot as a function of voltage over time. Figure 4-14 depicts the same data points captured in Figure 4-13 but plot as a function of frequency using the Fast Fourier Transform Algorithm. For the DOE parameters used during this weld sequence, reference Table 4-4. For baseline control results yielded by the Tessonics Ultrasonic Inspection unit, reference Table 4-5.

Electrical Signature Analysis of a Failing Performance: **Weld #3**

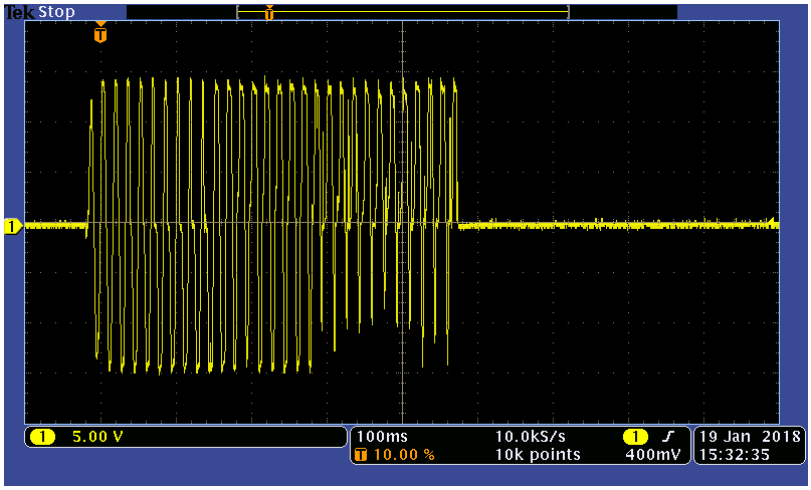

Figure 4-13: Weld 3 Electrical Sin Wave

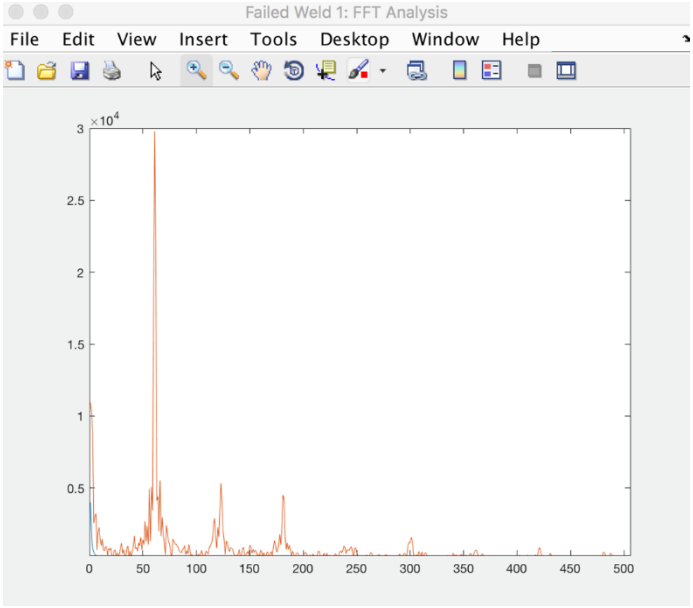

Figure 4-14: Weld 3 FFT Plot

Analyzing the electrical data of Weld 3 and the other welds deemed as no good, it becomes evident that the FFT performed on these welds yields almost identical results as the welds classified as good. Once again, there are four peak frequencies for all welds occurring at 0.5Hz, 31Hz, 62Hz & 91Hz respectively. This indicates that there is little to no change in the peak frequencies of welds classified as passing versus failed. However, a distinction may still be made from these plots. Although the welds classified as no good yield the same peaks as those classified as good, amongst those peaks lay an increase in smaller scattered peaks with a magnitude between 0 and 1,000. These smaller peaks or displacements are highlighted in Figure 4-15 below. The small scattered peaks themselves will be deemed infinitesimal for this research purpose simply because they are not substantial enough to build a repeatable relationship.

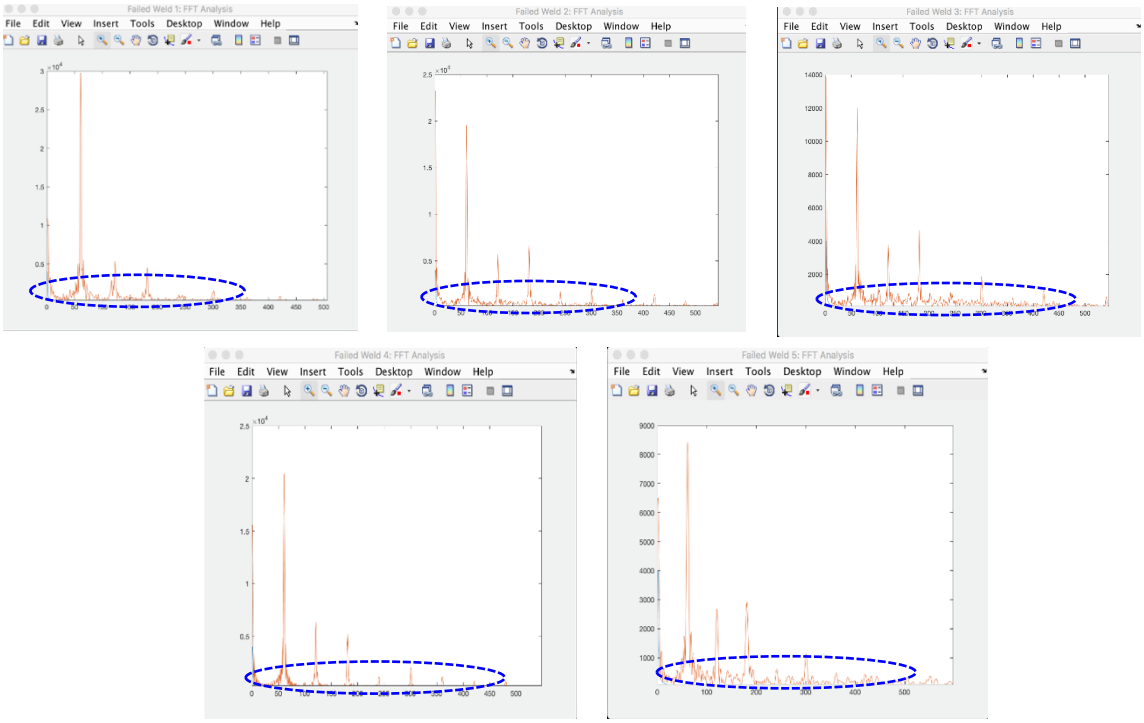

Figure 4-15: Fast Fourier Transform Plot: Welds 3, 9, 13, 25 & 31

That being the case, the correlation discovered within the electrical aspect of this research was not as profound as expected. The ultimate goal was to discover a relationship significant enough between good and bad welds that may be used as a training example for continuous improvement in the form of machine learning. Potential reasoning for this similar condition between passed and failed welds electrically is because of the consistent amount of current being sent to the electrodes during each weld sequence. Using the stationary 230V Miller Welder provided no ability to adjust power levels throughout the research trials. That being the case, the current passing through the electrode where the oscilloscope lay may be relatively consistent each time regardless of the quality output of the weld. This result closely resembles the study of electrical

signatures in the form of Dynamic Resistance referenced in Chapter 2 in which the graphical representation between good and bad welds behaved similarly.

An opportunity is still present however to compare the additional chatter identified in the Electrical FFT analysis to the peak frequency identified in the acoustic Spectrum Frequency Analysis Graph. Both calculations may be programmed into the PLC of a resistance spot welding robot. With both a sound recorder feeding the raw acoustic data and the robot transformer feeding the raw electrical data to the PLC, the calculations may be performed almost instantaneously comparing both characteristics and classifying the quality of the previous weld. This represents a relatively low-cost and still effective way to identify resistance spot weld quality at the source without an intricate apparatus or disruption to manufacturing processes.

CHAPTER 5. **STATISTICAL ANALYSIS SUMMARY**

For better visualization of the final results of all welds, the data was gathered and plot against each other to distinguish the correlations. While there were several different cases that resulted in a failed weld, (blowout, cold weld, undersized) all failed welds were classified as a data point 2 while all passed welds were classified as a data point 1. The first statistical summary presented is the comparison of the acoustic frequency data points to the pass/fail data points of each weld. The highlighted section in figure 5-1 below dictates the strong correlation between the failed welds and the higher peak frequency as discussed previously. This is due to the presence of additional sound in the form of data points captured when recording a weld failure such as a blowout with additional spatter. While there are a few outlying points, the trend here still proves a strong correlation between weld quality and acoustic feedback.

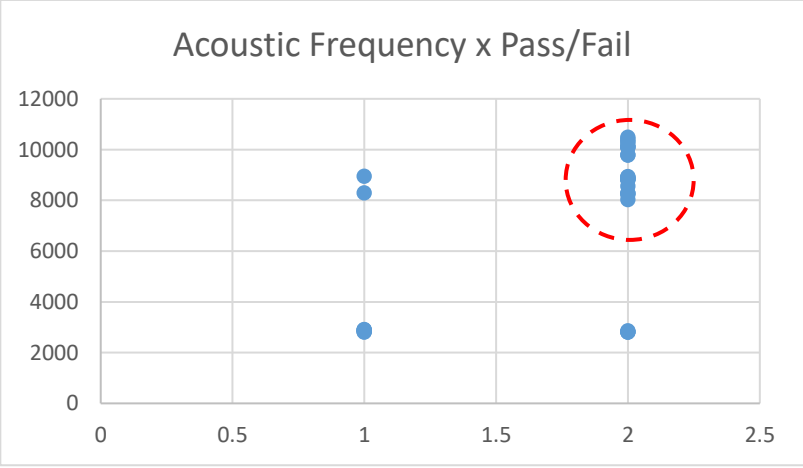

Figure 5-1: Acoustic Frequency x Pass/Fail

The second statistical summary compares the same pass/fail data points of each weld to the frequency analysis calculated from the electrical signature of each weld. Unlike the acoustic comparison, Figure 5-2 below portraits less of a correlation between the pass/fail data points and the electrical frequency data points. As discovered in Chapter 4, all welds yielded peak electrical frequencies of either 0.5Hz or 31Hz**.** This occurred across both passing and failing welds resulting in all data points being stacked on top of each other in the four locations shown.

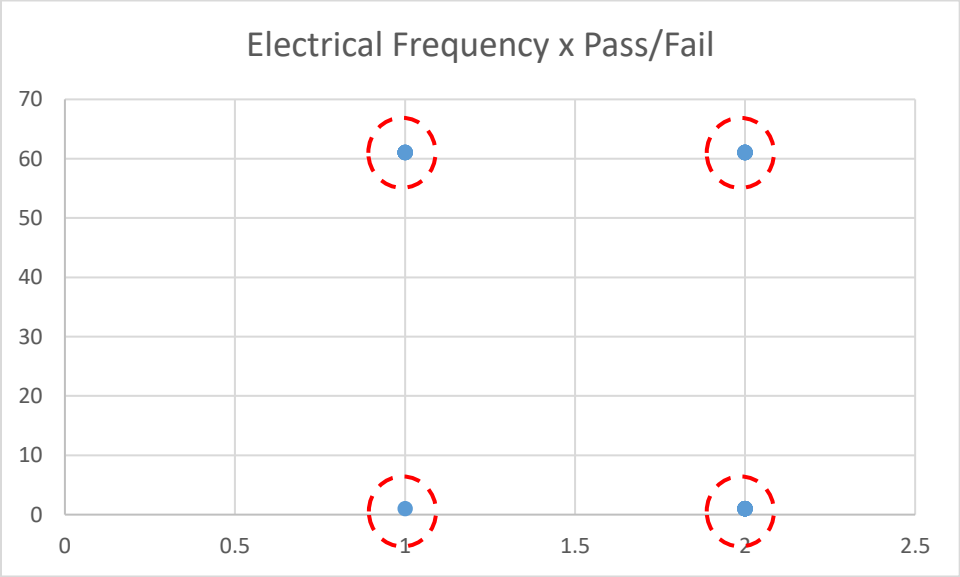

Figure 5-2: Electrical Frequency x Pass/Fail

The third statistical summary performed is a combination of the previous two. It takes the both the electrical frequency and acoustic frequency data points and plots them as a function of each other to discover a correlation. Figure 5-3 below summarizes the acoustic frequency data points as the y-axis data points while the electrical frequency data points serve as the x-axis values. Similar to the electrical frequency statistical analysis, there is not a strong correlation between the data points as most are clustered at

different points of the graph. There are instances in which welds with larger acoustic peak frequencies correlate with the welds that possess larger electrical peak frequencies and vice versa.

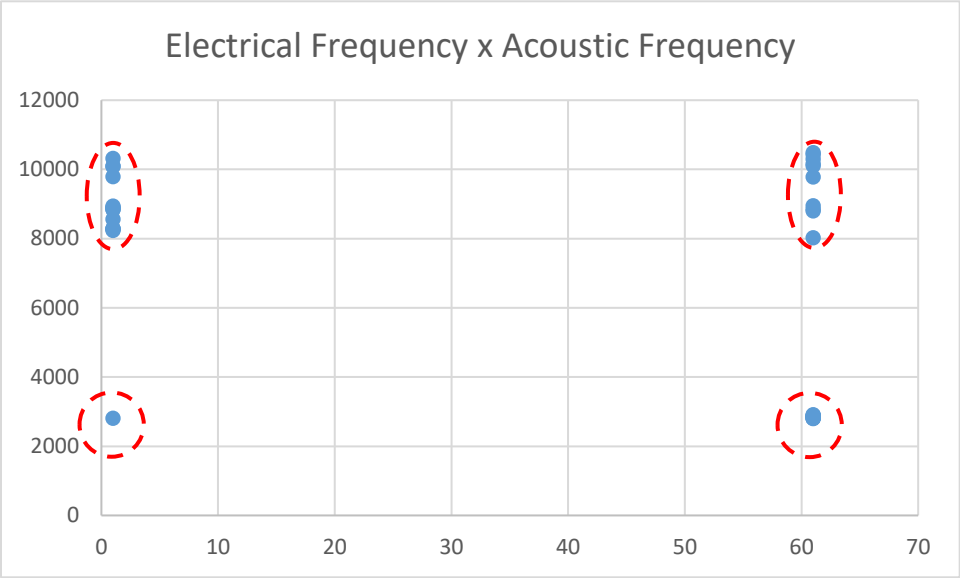

Figure 5-3: Acoustic Frequency x Electrical Frequency

Based on the statistical summaries, it becomes evident that the most prominent correlation present is between the acoustic peak frequencies and the pass/fail data points of each weld. Although the electrical frequency data did not display a significant correlation statistically, the data may still be used to distinguish welds by increasing visibility on the minimal frequency peaks present during failed welds. This additional layer of granularity coupled with the distinguished acoustic peak frequency correlation presents an opportunity for additional methods of classifying weld quality at the source.

CHAPTER 6. **CONCLUSION**

The objective of this research was to identify a correlation between two different characteristics within the weld sequence that allow the quality of a weld to be determined in-process. This correlation would then allow for 100% weld confirmation at the source increasing both process efficiency and product quality. The data captured and analyzed shows a visible correlation between weld quality and the acoustic emissions produced. The comparison of electrical signatures to weld quality however was not as prominent. The fidelity of the equipment used may be one underlying reason for a trend not showing as expected. A more intricate setup with the ability to capture additional data points at lower levels may be required to highlight a correlation between electrical signatures and weld quality, in particular the additional peak frequencies identified in failing welds. The acoustic correlation however was still very distinguished and may be built upon moving forward to increase efficiency and product quality in welding processes.

The contributions of this research to the field still prove useful. Utilization of both acoustic and electrical feedback provide a more sound method of identifying weld nugget quality than simply a single parameter analysis. The use of the Fast Fourier transform algorithm as well, serves as a contribution for further work; allowing for additional weld sequence characteristics to be researched and measured as functions of frequency. Ultimately this will result in the discovery of additional parameters that may have an impact on weld nugget quality and how they may be monitored in-process.

6.1 MACHINE LEARNING & FURTHER RESEARCH

Machine Learning is the field of study that gives computers the ability to learn without being explicitly programmed. Using a large sum and variety of training examples, an algorithm may be written to improve the performance of a machine over time. In this scenario, the theory is to take the correlation discovered here acoustically and input that framework into a standard spot weld robot controller. By programming the range in which weld parameters may be adjusted based on feedback, the Programmable Logic Controller (PLC) has the opportunity to learn from itself over time. In many high-volume manufacturing applications, robots have the ability to compensate for constant variation such as tip wear and panel gaps. In parallel, if the peak frequency of each weld can be captured and measured during the weld sequence, the robot can respond in two ways. The first action would be sending feedback to the station controller of that process to flag the specific weld or welds that exceed the threshold of what was trained acceptable as a good weld. The second action would be to adjust parameters based on that result to improve the condition during the next cycle. Due to the variety of parameters that may be adjusted, such as pressure, current, squeeze time, etc., an excess of 10,000 training samples will be required to effectively teach the program which parameter should be adjusted based on the output.

Beyond just the machine learning application, this research can be furthered in other ways. One particular instance can be outside of resistance spot welding and within the realm of arc welding. Traditionally, arc/mig welding produces much higher acoustic emissions due to the external laying of the weld bead between sheets. Exploring this would present even more intricate sound waves to research and correlate with electrical

signatures. Although RSW applications are more prominent in high volume manufacturing processes, the impact of identifying the correlation within arc welding may be just as beneficial. The difference lays within the repair of an arc weld versus the repair of a spot weld. Re-welding a spot weld often has an adverse effect resulting in the continued decrease in the quality of the weld. Re-Welding an arc weld however which is often required to be done manually if not sufficiently completed in line can be done with no negative impact to the quality of the weld, only strengthening it. This presents an opportunity for a robot in-line that makes a poor arc weld to circle back and repair the same weld at the source prior to shipping it downstream.

Based on the research conducted, it has become evident that there is a certain level of correlation between the acoustic and electric emission of a spot weld in relation to its quality. While the distinction discovered when analyzing the electrical signature was deemed negligible, there is still an opportunity here to further the research by examining a different generation of spot welder or oscilloscope that provides additional granularity. Doing so may allow for a more detailed retention of electrical sin waves from the weld gun electrode resulting in a more prominent correlation. Further recommendations on how this research can be furthered are greatly welcomed in anticipation that this concept continues to move forward from the research and development phase to full scale implementation in a high-volume manufacturing facility.

[APPENDIX A. PASSING WELD RESULTS]

Weld #6

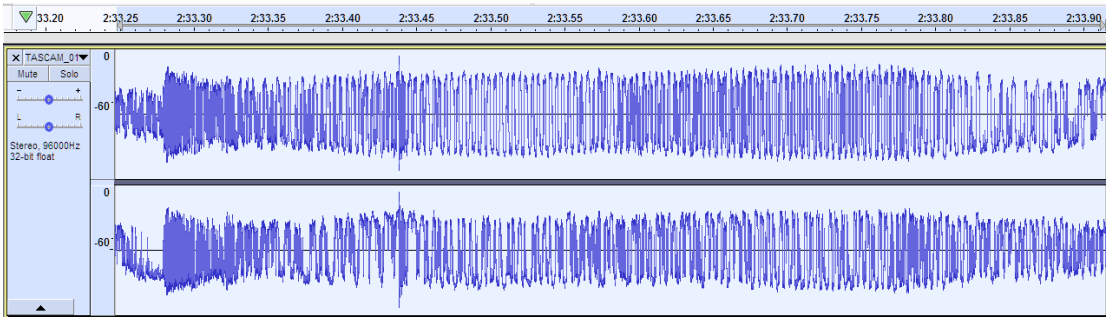

Figure A-1:Weld 6 Acoustic Sin Wave

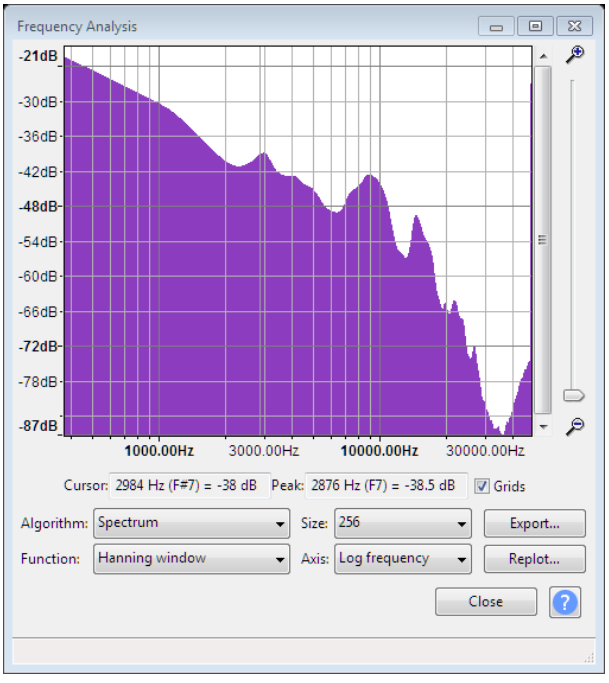

Figure A-2: Weld 6 Spectrum Frequency Analysis Graph

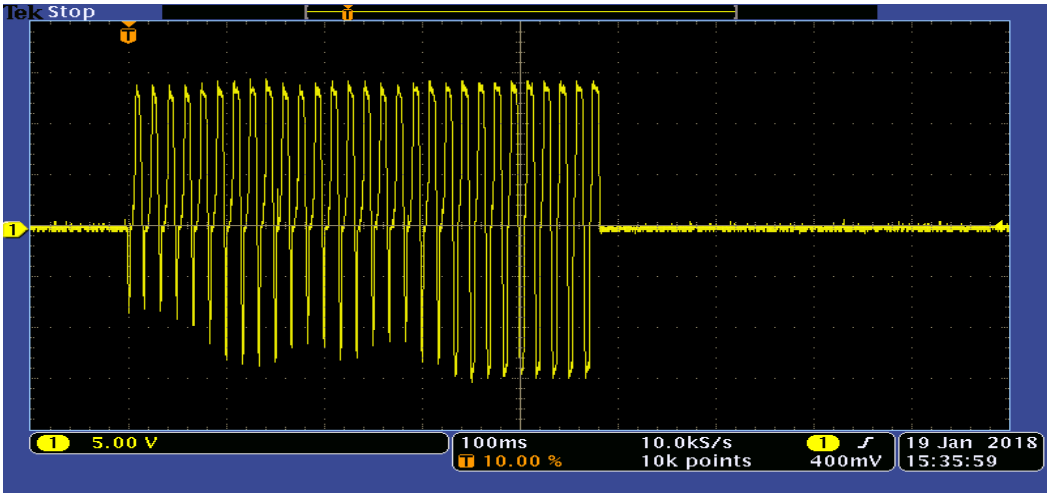

Figure A-3: Weld 6 Electrical Sin Wave

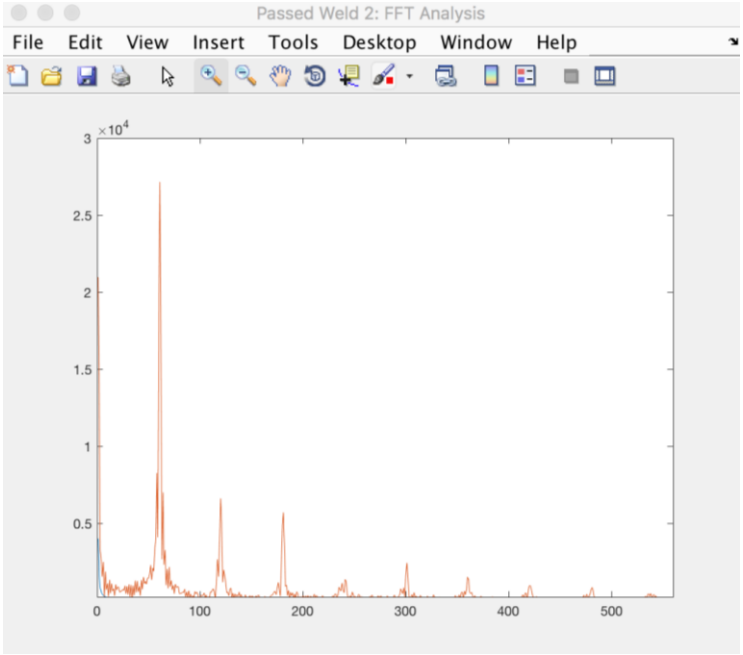

Figure A-4: Weld 6 FFT Plot

Table A-1: Weld 6 DOE Parameters

Material	Pressure	Weld Time
A x A (1.0mm)	Heavy (30 lbs)	0.5 seconds.

Table A-2: Weld 6 Ultrasonic Inspection Results

Decision		Weld	Diameter		Classification	C-Scan
Pass/Fail	Reason	ID	Required (A-Class)	Measured	A,B,C, Cold	
Pass	-	Weld006	5	4.1	B Class	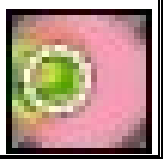

Weld #10

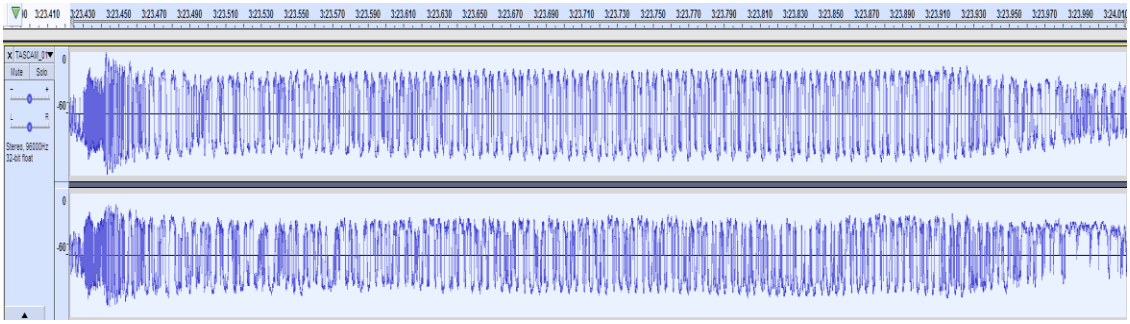

Figure A-5: Weld 10 Acoustic Sin Wave

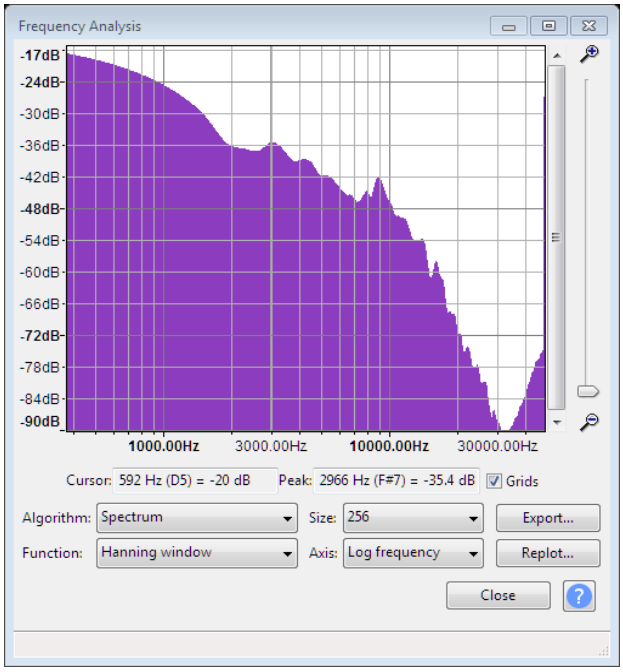

Figure A-6: Weld 10 Spectrum Frequency Analysis Graph

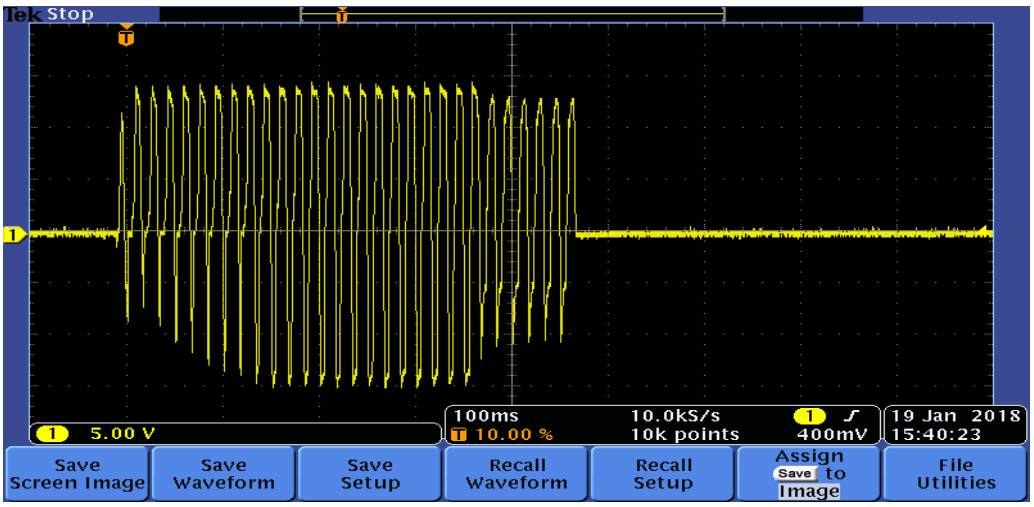

Figure A-7:Weld 10 Electrical Sin Wave

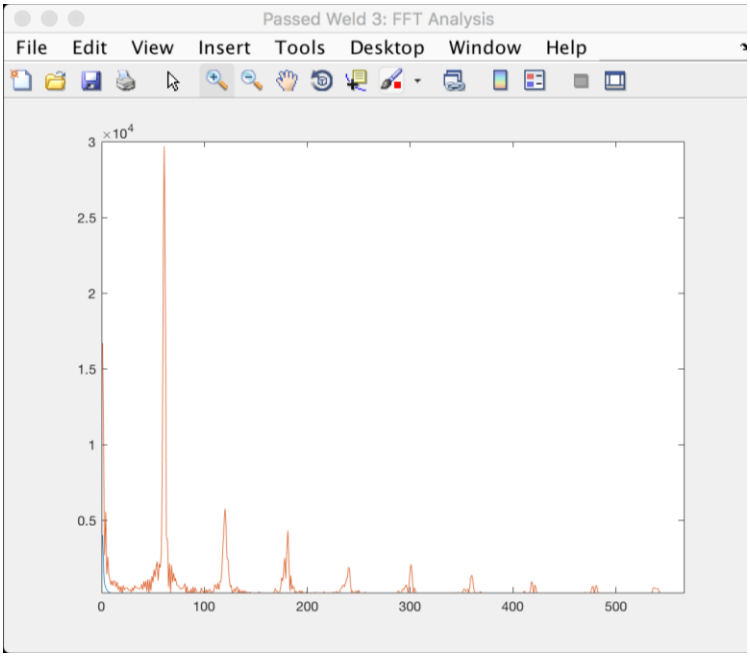

Figure A-8: Weld 10 FFT Plot

Table A-3: Weld 10 DOE Parameters

Material	Pressure	Weld Time
B x B (0.5mm)	Heavy (30 lbs)	0.5 seconds.

Table A-4: Weld 10 Ultrasonic Inspection Results

Decision		Weld	Diameter		Classification	C-Scan
Pass/Fail	Reason	ID	Required (A-Class)	Measured	A,B,C, Cold	
Pass	-	Weld010	3.5	3.4	B Class	

Weld #32

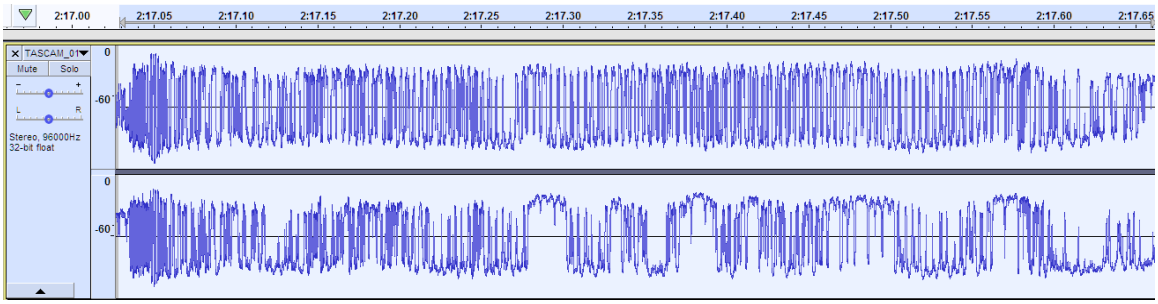

Figure A-9: Weld 32 Acoustic Sin Wave

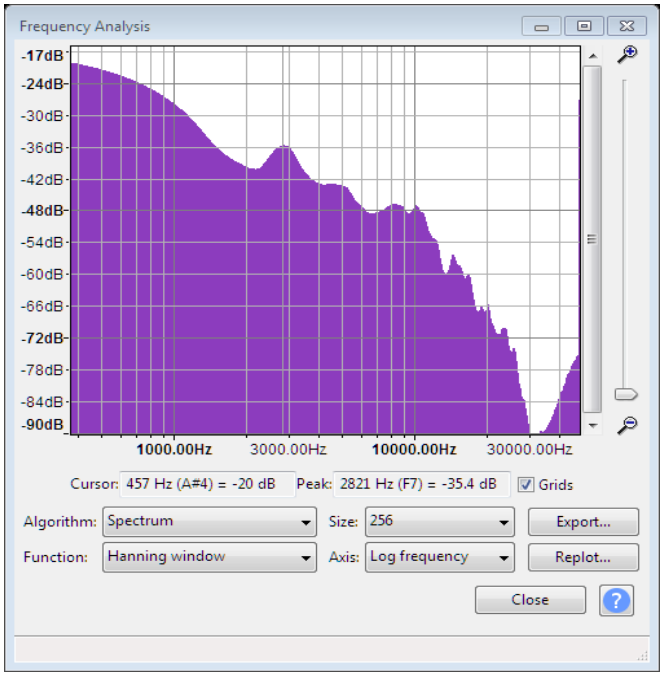

Figure A-10: Weld 32 Spectrum Frequency Analysis Graph

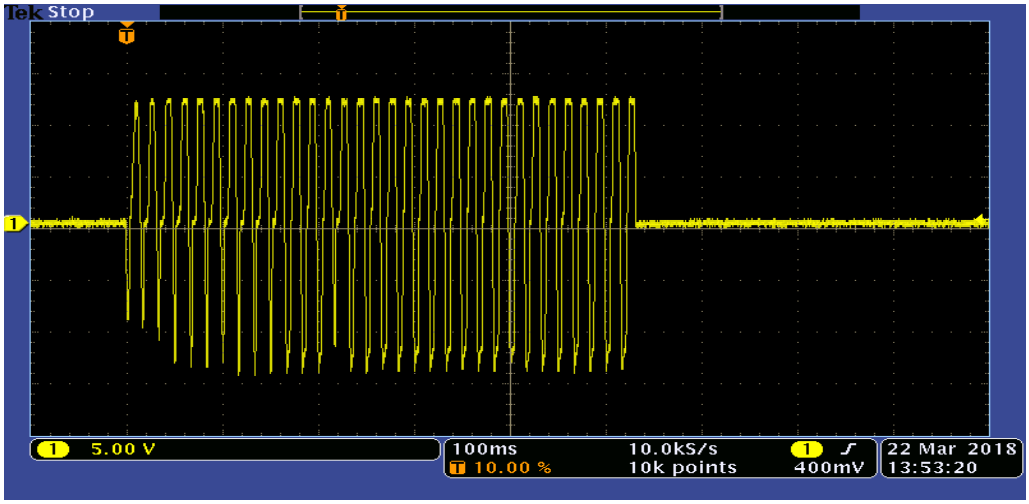

Figure A-11: Weld 32 Electrical Sin Wave

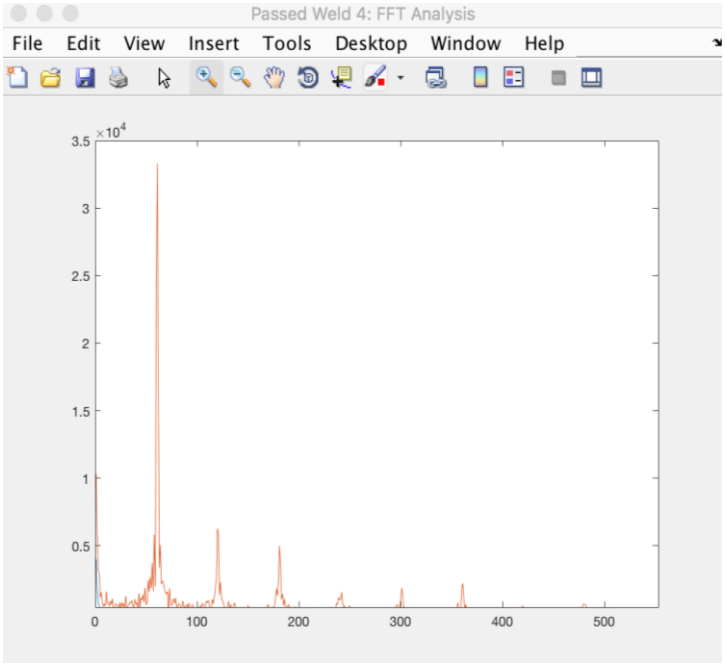

Figure A-12: Weld 32 FFT Plot

Table A-5: Weld 32 DOE Parameters

Material	Pressure	Weld Time
A x B (1.0 x 0.5mm)	Heavy (30 lbs)	0.5 seconds.

Table A-6: Weld 32 Ultrasonic Inspection Results

Decision		Weld	Diameter		Classification	C-Scan
Pass/Fail	Reason	ID	Required (A-Class)	Measured	A,B,C, Cold	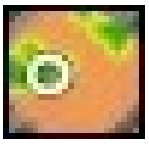
Pass	-	Weld032	3.5	2.9	B Class	

Weld #34

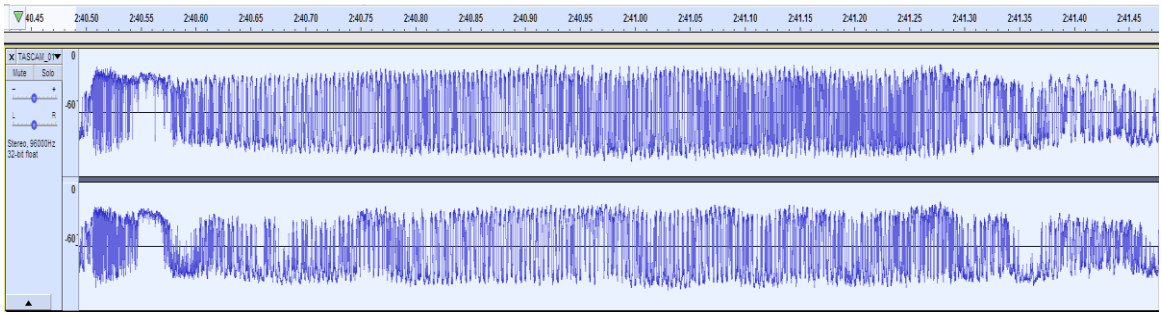

Figure A-13: Weld 34 Acoustic Sin Wave

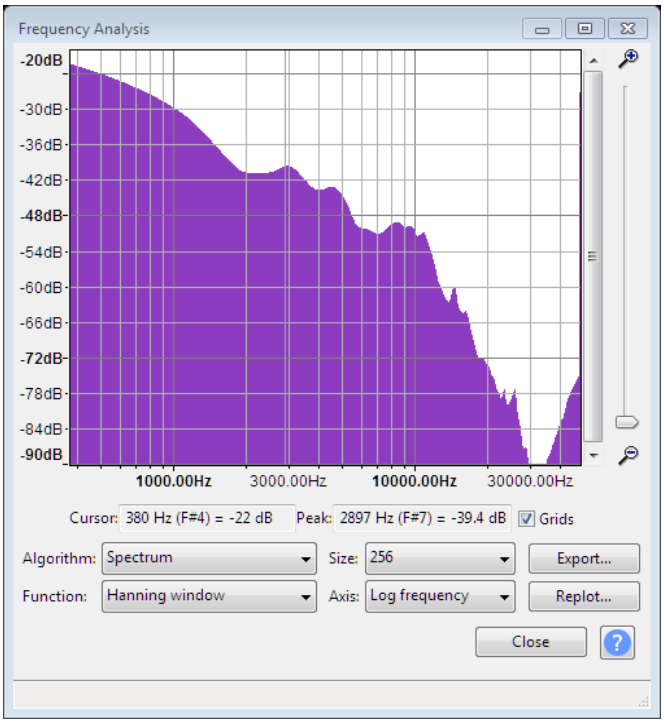

Figure A-14: Weld 34 Spectrum Frequency Analysis Graph

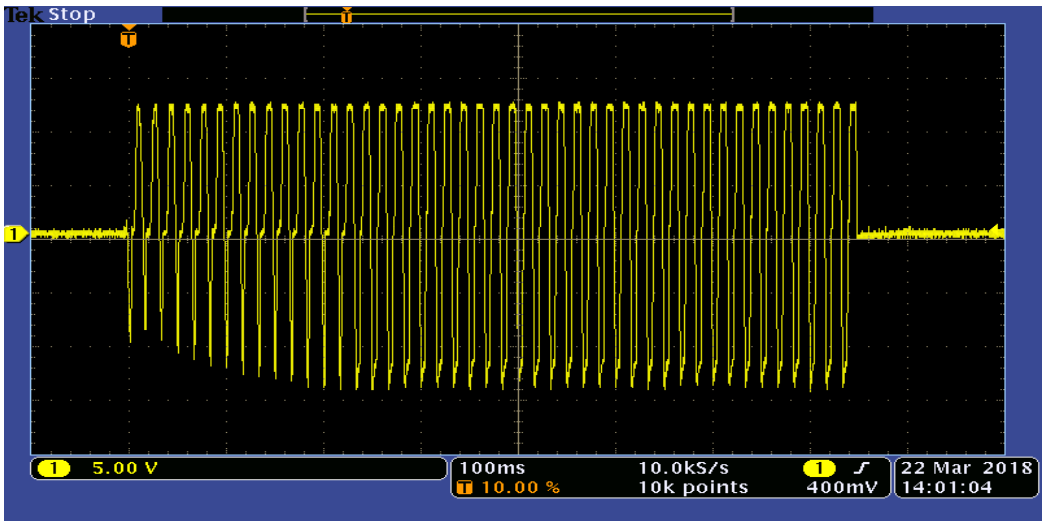

Figure A-15: Weld 34 Electrical Sin Wave

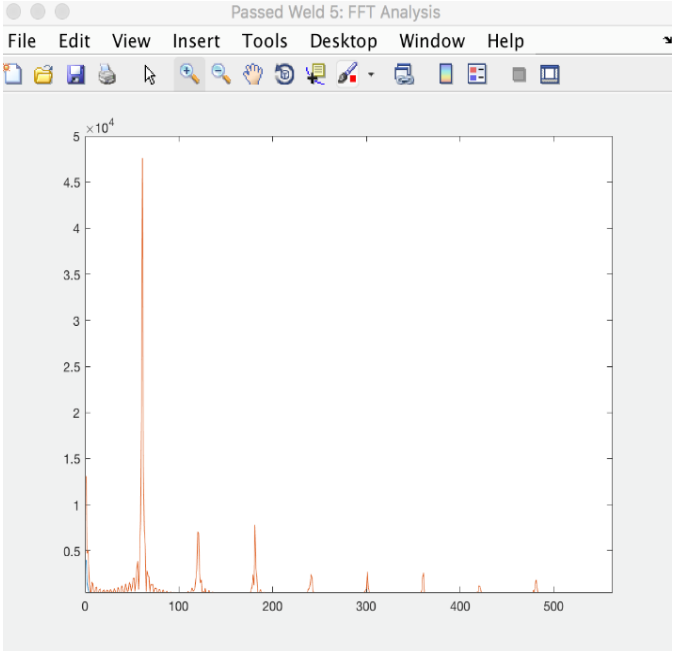

Figure A-16: Weld 34 FFT Plot

Table A-7:Weld 34 DOE Parameters

Material	Pressure	Weld Time
B x B (0.5mm)	Heavy (30 lbs)	0.7 seconds.

Table A-8: Weld 34 Ultrasonic Inspection Results

Decision		Weld	Diameter		Classification	C-Scan
Pass/Fail	Reason	ID	Required (A-Class)	Measured	A,B,C, Cold	
Pass	-	Weld034	3.5	2.8	B Class	

[APPENDIX B. FAILED WELD RESULTS]

Weld #9

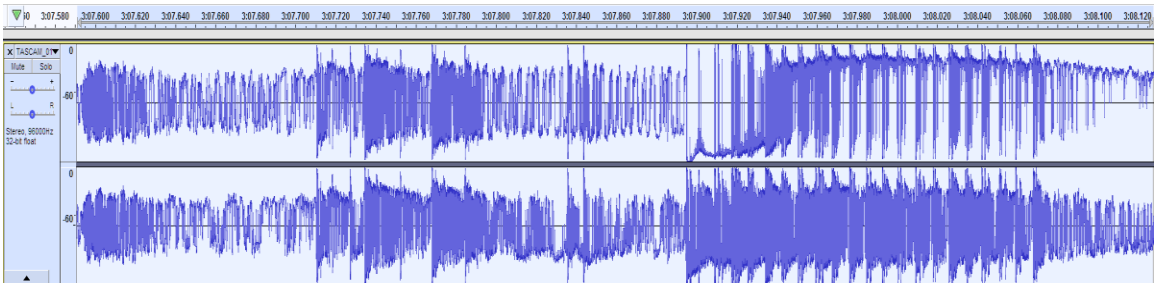

Figure A-17: Weld 9 Acoustic Sin Wave

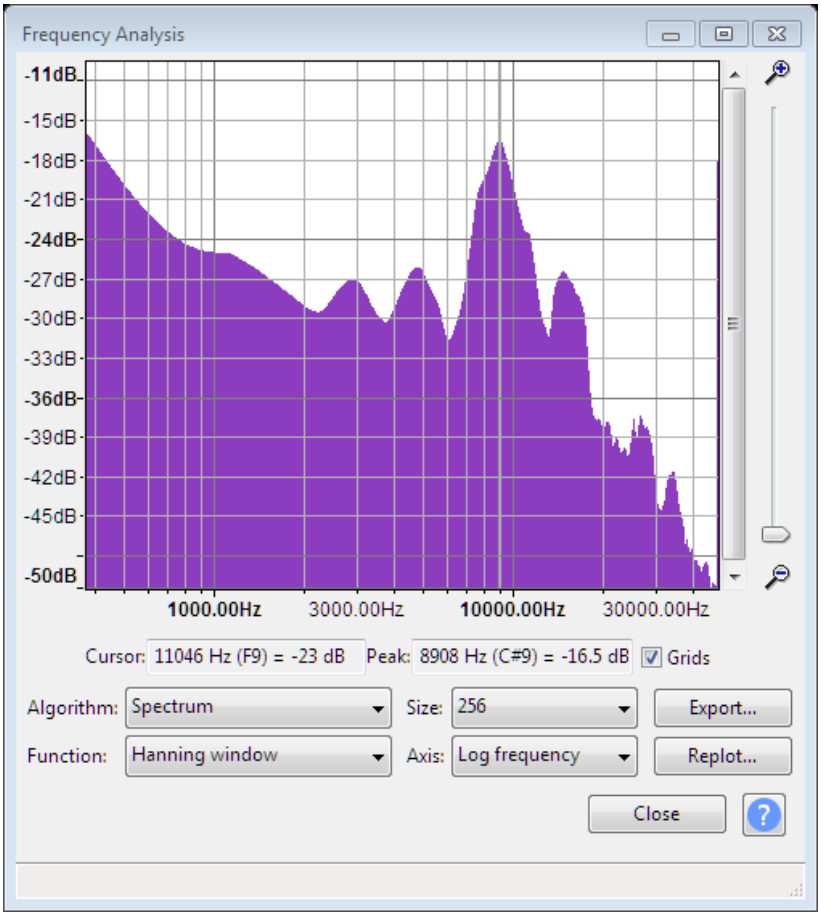

Figure A-18: Weld 9 Spectrum Frequency Analysis Graph

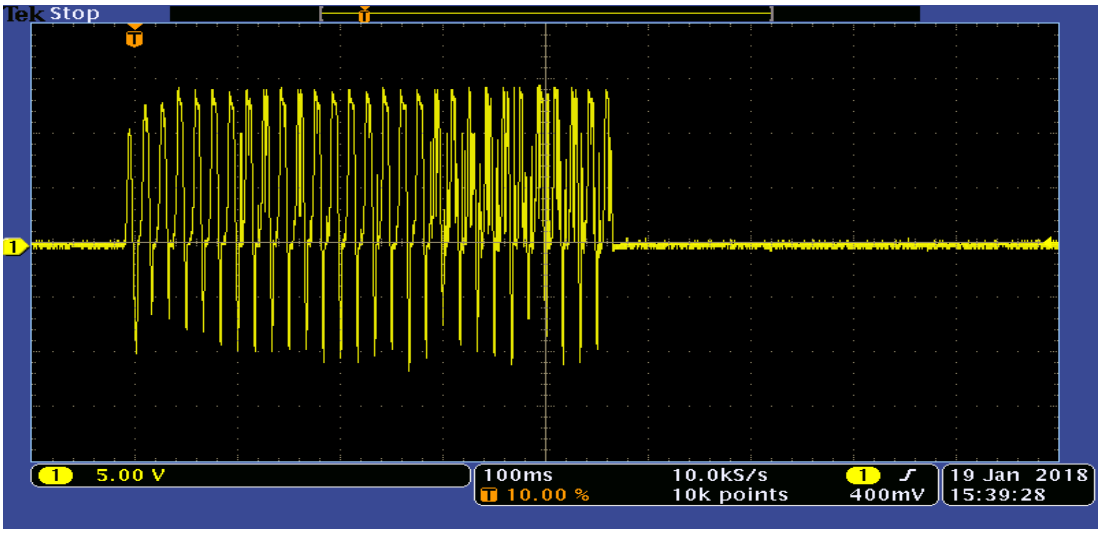

Figure A-19: Weld 9 Electrical Sin Wave

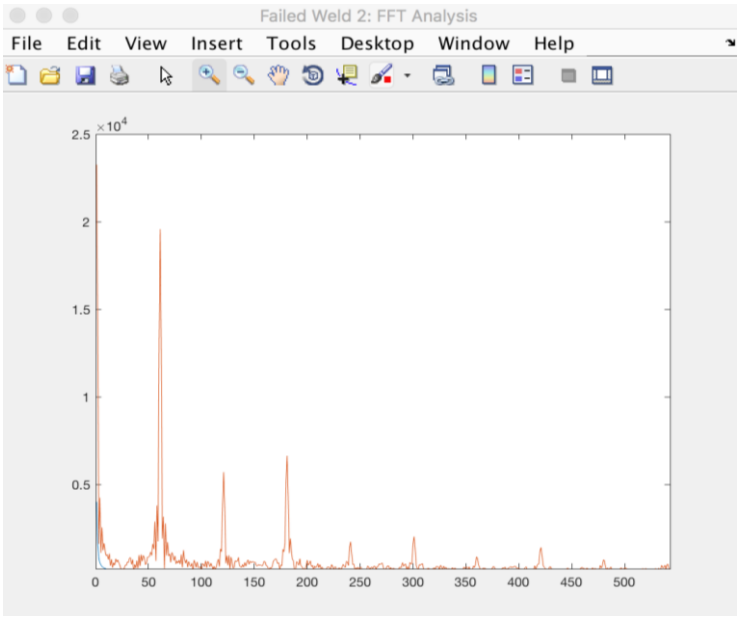

Figure A-20: Weld 9 FFT Plot

Table A-9: Weld 9 DOE Parameters

Material	Pressure	Weld Time
B x B (0.5mm)	Heavy (30 lbs)	0.5 seconds.

Table A-10: Weld 9 Ultrasonic Inspection Results

Decision		Weld	Diameter		Classification	C-Scan
Pass/Fail	Reason	ID	Required (A-Class)	Measured	A,B,C, Cold	
Fail	RSW Pinhole	Weld009	3.5	N/A	Pinhole	

Weld #13

Figure A-21: Weld 13 Acoustic Sin Wave

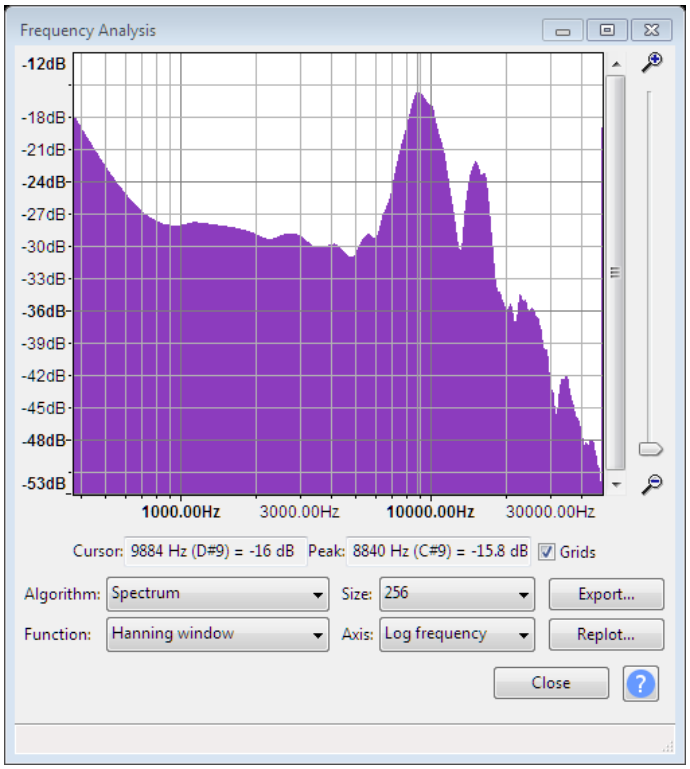

Figure A-22: Weld 13 Spectrum Frequency Analysis Graph

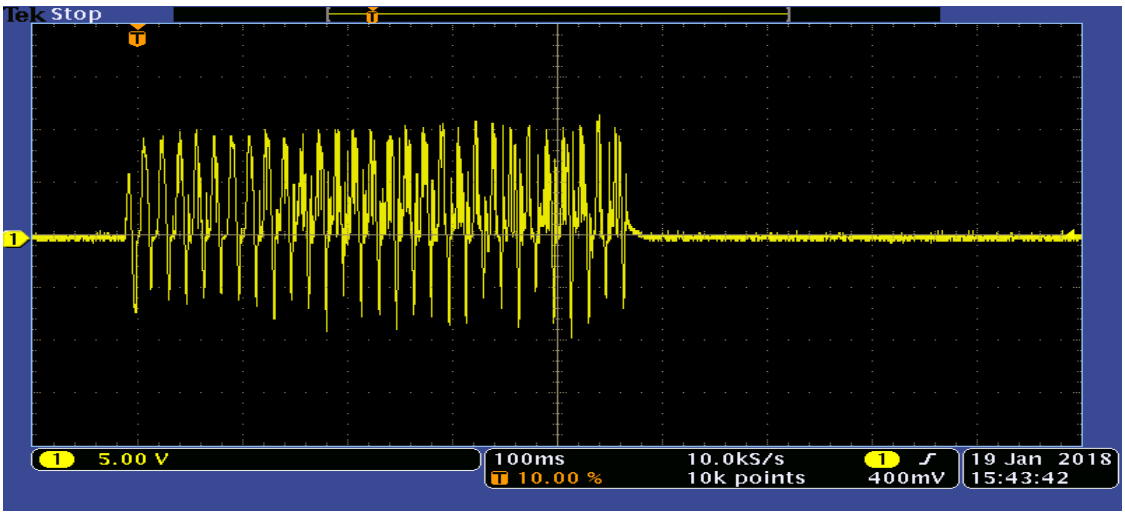

Figure A-23: Weld 13 Electrical Sin Wave

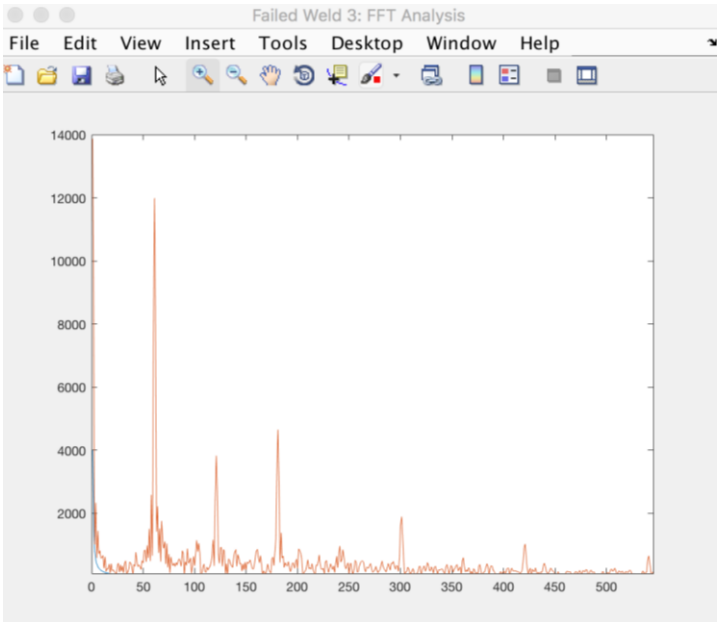

Figure A-24: Weld 13 FFT Plot

Table A-11: Weld 13 DOE Parameters

Material	Pressure	Weld Time
B x B (0.5mm)	Light (20 lbs)	0.5 seconds.

Table A-12: Weld 13 Ultrasonic Inspection Results

Decision		Weld	Diameter		Classification	C-Scan
Pass/Fail	Reason	ID	Required (A-Class)	Measured	A,B,C, Cold	
Fail	RSW Cold	Weld013	3.5	N/A	Cold	

Weld #25

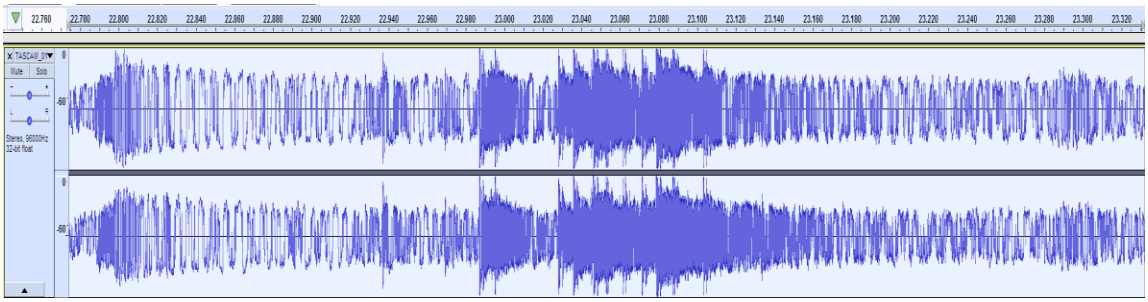

Figure A-25: Weld 25 Acoustic Sin Wave

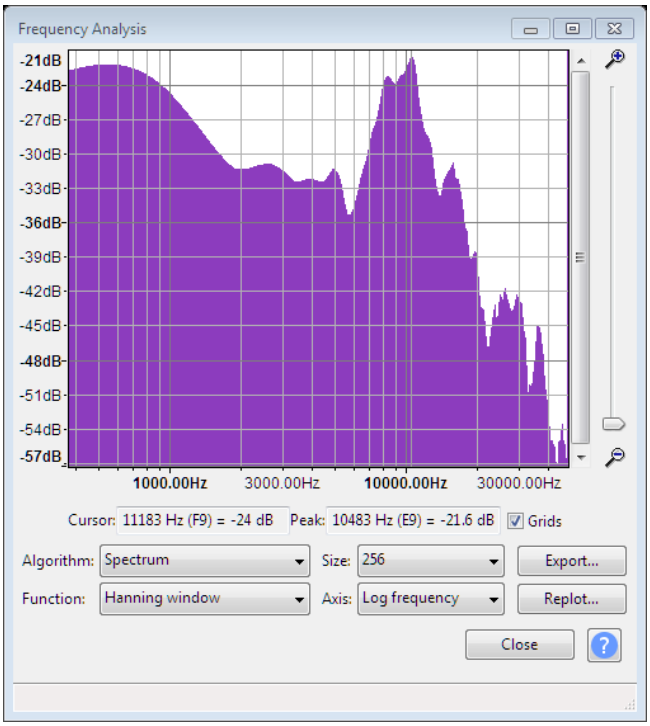

Figure A-26: Weld 25 Spectrum Frequency Analysis Graph

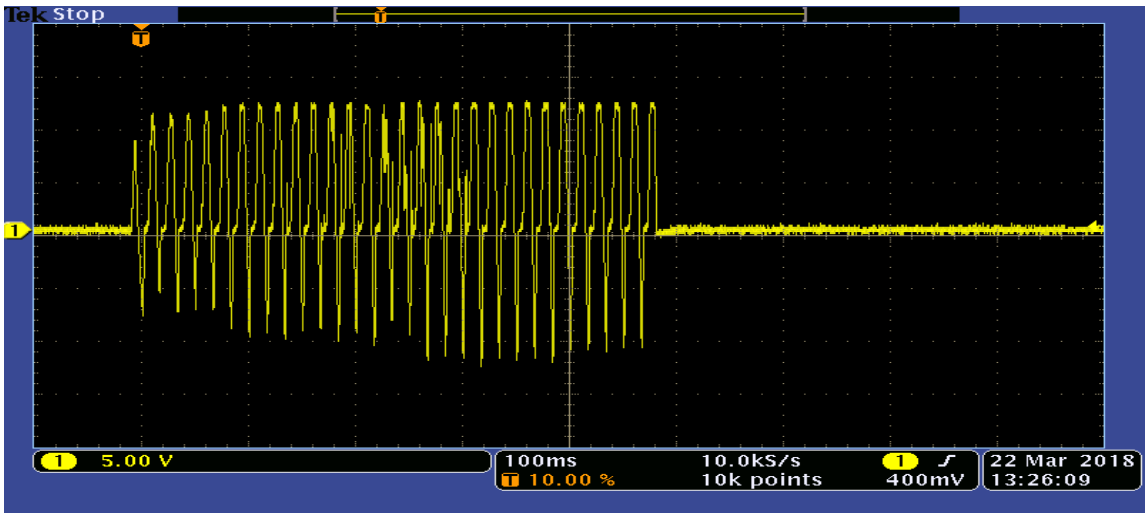

Figure A-27: Weld 25: Electrical Sin Wave

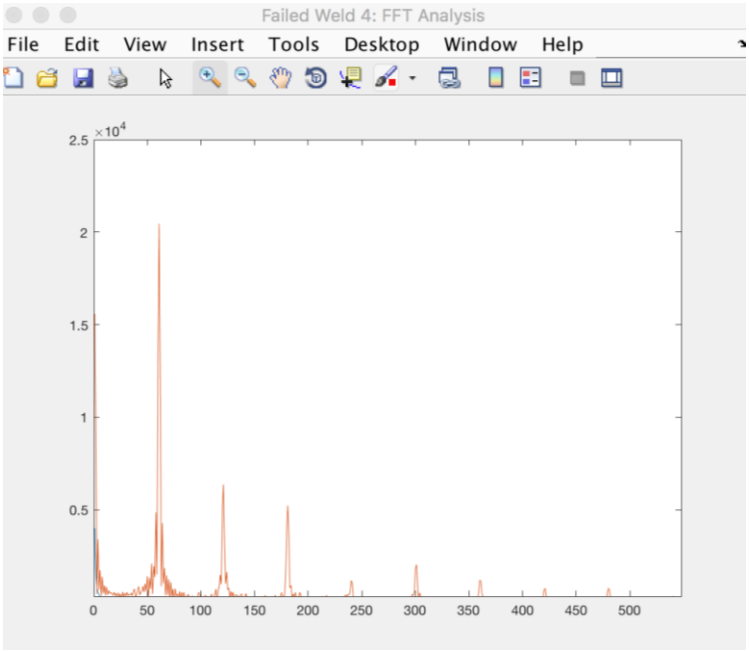

Figure A-28: Weld 25 FFT Plot

Table A-13:Weld 25 DOE Parameters

Material	Pressure	Weld Time
A x A (1.0 mm)	Light (20 lbs)	0.5 seconds.

Table A-14: Weld 25 Ultrasonic Inspection Results

Decision		Weld	Diameter		Classification	C-Scan
Pass/Fail	Reason	ID	Required (A-Class)	Measured	A,B,C, Cold	
Fail	RSW Undersized	Weld025	5	2.7	C Class	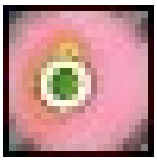

Weld #31

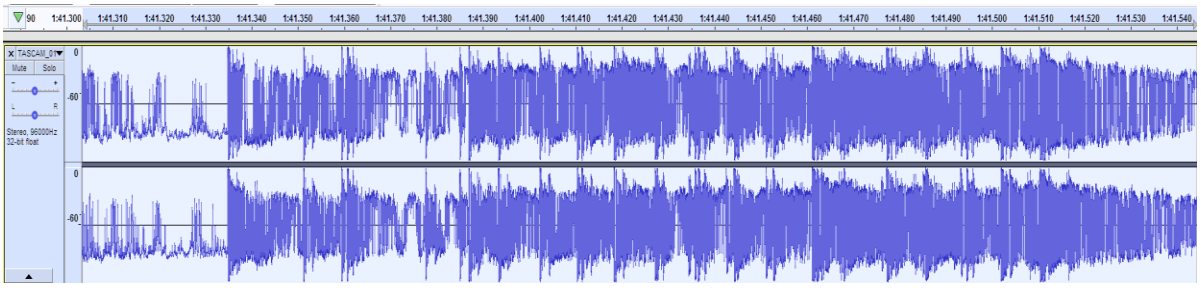

Figure A-29: Weld 31 Acoustic Sin Wave

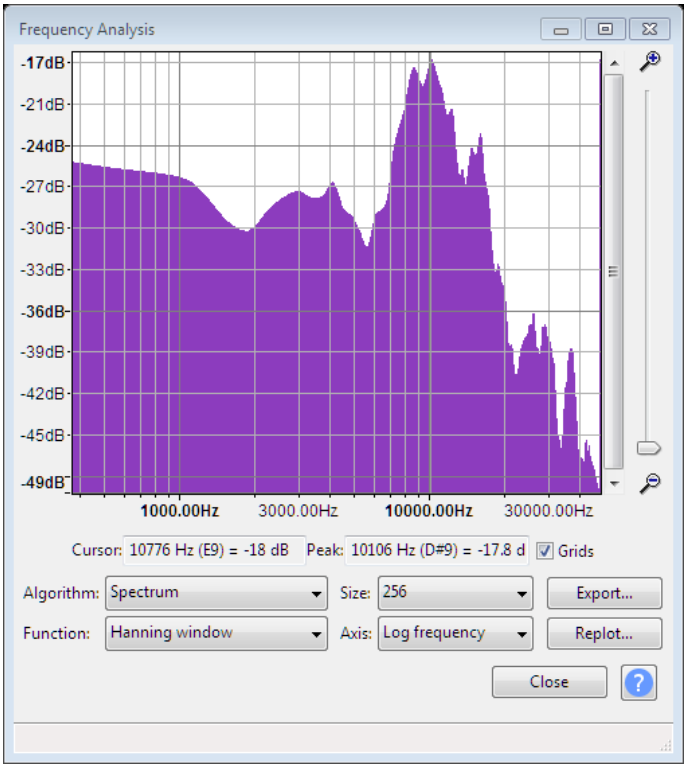

Figure A-30: Weld 31 Spectrum Frequency Analysis Graph

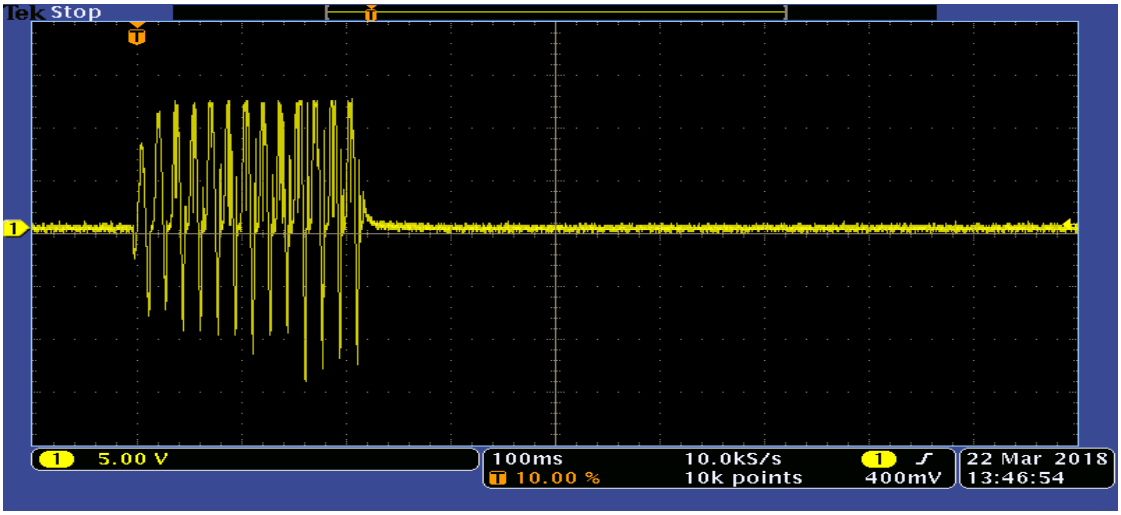

Figure A-31: Weld 31 Electrical Sin Wave

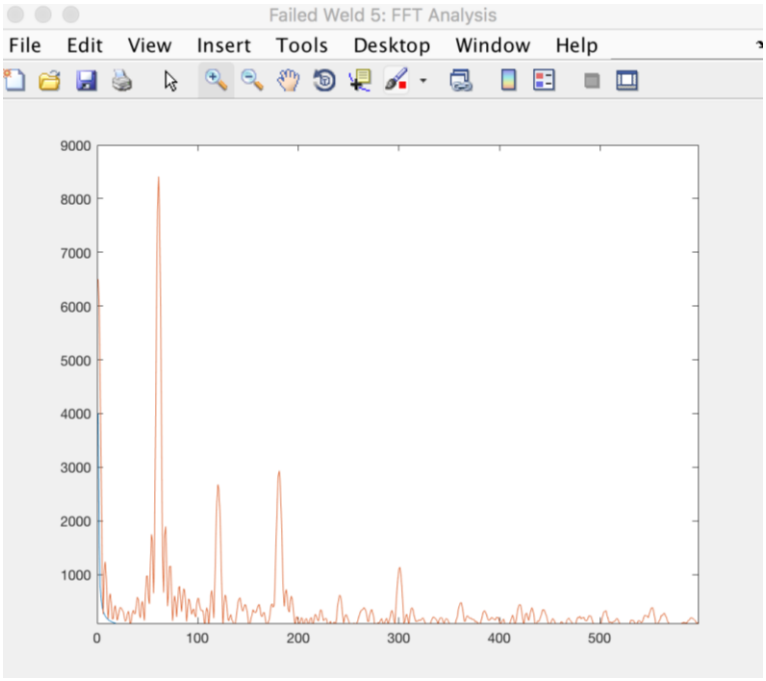

Figure A-32: Weld 31 FFT Plot

Table A-15:Weld 31 DOE Parameters

Material	Pressure	Weld Time
B x B (0.5 mm)	Light (20 lbs)	0.5 seconds.

Table A-16:Weld 31 Ultrasonic Inspection Results

Decision		Weld	Diameter		Classification	C-Scan
Pass/Fail	Reason	ID	Required (A-Class)	Measured	A,B,C, Cold	
Fail	RSW Undersized	Weld031	3.5	2.5	C Class	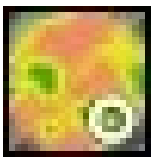

REFERENCES

[1] Al Jader, M.A. (2014). Investigation of Spot Welding Electrode Tip Wear And A Non-Destructive Test of Plastic Joining in the Automotive Industry. PhD Dissertation, *Liverpool John Moores University*, *pp 19-23*

[2] Al Jader, M.A., Cullen, J.D., Al-Shamma'a, A.I., & Wylie, N. (2010). Investigation Into Spot Welding Process Sustainability For the Automotive Industry. *Liverpool John Moores University, RF & Microwave Group, Byrom Street, Liverpool, L3 3AF, pp 34-41*

[3] AlcoTec. (2015). *Destructive Testing of Welds* Retrieved, February 3, 2019, from http://www.alcotec.com/us/en/education/knowledge/weldinginspection/Destructive-Testing-of-Welds.cfm

[4] Amada Miyachi America. (2016). *Weld Nugget* Retrieved, October 21, 2018, from http://www.amadamiyachi.com/glossary/glossweldnugget

[5] Batalha, G.F., Stocco, D., & Vilela, D. (2012). Spot weld fatigue durability performance evaluation through the use of Finite Elements Analysis & Design for Life Cycle. *Open Access Library Volume 6 (12)*, *pp 68-85*

[6] Brand, M. J., Jossen, A., Schmidt, P. A., & Zaeh, M. F. (2015). Welding techniques for battery cells and resulting electrical contact resistances. *Journal of Energy Storage, Volume 1, pp 7-14*

[7] The United States Bureau of Transportation Statistics. (2016). *Average Age of Automobiles and Trucks in Operation in the United States* Retrieved, October 21, 2018, from https://www.bts.gov/content/average-age-automobiles-and-trucks-operation-united-states

[8] Chen, C.H., Han, Z., Indacochea, J.E., & Orozco, J. (1989). Resistance Spot Welding: A Heat Transfer Study. *Welding Research Supplement, 9 pages*

[9] Chertov, A.M., Maev, R.Gr. (2004). Determination of Resistance Spot Weld Quality in Real Time Using Reflected Acoustic Waves. Comparison With Through-Transmission Mode. *University of Windsor, Windsor, Ontario, Canada, 8 pages*

[10] Cho, Y., Rhee, S. (2000). New technology for measuring dynamic resistance and estimating strength in resistance spot welding. *Measurement Science & Technology, Vol. 11, pp 1173-1178*

[11] Dai, W.L., Dickinson, D.W., Papritan, J.C., & Tsai, C.L. (1991) Analysis and Development of a Real-Time Control Methodology in Resistance Spot Welding. *SAE Technical Paper, 14 pages*

[12] Enami, M. (2016). Evaluation of mechanical properties of Resistance Spot Welding and Friction Stir Spot Welding on Aluminum Alloys. *University of Tehran, Tehran, Iran, 12 pages*

[13] Esmail, E. A., Grum, J., & Polajnar, I., (2008). Sources of Acoustic Emission In Resistance Spot Welding. *University of Ljubljana, Slovenia, Alexandria University, Egypt, 8 pages*

[14] Ertas, A. H., Sonmez, F. O. (2008). A parametric study on fatigue strength of spot-weld joints. *Bogazici University, Istanbul, Bebek, 34342, Turkiye, 11 pages*

[15] Floyd, S., Saini, D. (1998). An Investigation of Gas Metal Arc Welding Sound Signature for On-Line Quality Control. *American Welding Society, Welding Journal 1998, 8 pages*

[16] Guo, Z., Fang, P., Cui, J., & Wang, J. (2012) A Study of Fuzzy Neural Networks Control for the Quality of Resistance Spot Welding *Applied Mechanics and Materials Vols. 117-119 (2012) pp 1888-1894*

[17] Harting-USA. (2008). Hall effect current sensors brochure

[18] Kang, Z. (2012). Development of an Online Quality Control System for Resistance Spot Welding. PhD Dissertation, *The Hong Kong University of Science & Technology, pp 26-125*

[19] Ling, S., Wan, L., Wong, Y., & Li, D. (2010). Input electrical impedance as quality monitoring signature for characterizing resistance spot welding. *NDT&E International 43 (2010), pp 200–205*

[20] Luo, Y., Li, J.L., & Wu, W. (2013). Nugget quality prediction of resistance spot welding on aluminum alloy based on structureborne acoustic emission signals. *Science & Technology of Welding & Joining. May 2013, Vol. 18 Issue 4, pp 301-306*

[21] Metal Supermarkets. (2015). *Which Metals Conduct Electricity* Retrieved, February 3, 2019, from https://www.metalsupermarkets.com/which-metals-conduct-electricity/

[22] Miller. (2018). Guidelines For Resistance Spot Welding *Owner's Record*

[23] Nied, H.A. (1984). The Finite Element Modeling of the Resistance Spot Welding Process. *American Welding Society Welding Journal 63, 10 pages*

[24] Pan, N., Sheppard, S. (2002). Spot welds fatigue life prediction with cyclic strain range. *International Journal of Fatigue Volume 24, Issue 5, pp 499-602*

[25] Power Guru. (2012). *Introduction to Closed Loop Hall Effect Current Transducers* Retrieved, October 21, 2018, from http://www.powerguru.org/closed-loop-hall-effect-current-transducers/

[26] Regalado, W. J. P. (2014). Ultrasonic Real-Time Quality Monitoring of Aluminum Spot Weld Process. PhD Dissertation, *University of Windsor, Windsor, Ontario, pp 25-139*

[27] Robot Welding. (2001). *Spot Welding Parameters* Retrieved, February 3, 2019, from http://www.robot-welding.com/Welding_parameters.htm

[28] Saleem, J. (2012). Power Electronics for Resistance Spot Welding Equipment. Master's Thesis, *Mid Sweden University Sundsvall, Sweden, 60 pages*

[29] Simulation Manufacturing. (2019). *Challenges In Resistance Spot Welding* Retrieved, February 3, 2019, from https://www.simufact.com/resistance-spot-welding.html

[30] Spot Welding Services. (2018). *Advantages of Spot Welding* Retrieved, March 1, 2018, from http://www.vista-industrial.com/spot-welding.php

[31] Tang, H. (2000). Machine mechanical characteristics and their influences on resistance spot welding quality. PhD Dissertation, *University of Michigan, Ann Arbor, MI, pp 19-76*

[32] Tite-Spot. (2019). *Spot Welding Technical Information* Retrieved, February 3, 2019, from https://www.titespot.com/spot-welding-technical-information/

[33] Tessonics Corp. (2008). *Real-Time In-Line Spot Weld Analyzer Specification Sheet* Retrieved, October 21, 2018, from http://www.tessonics.com/files/riwa/RIWA-Spec-en.pdf & http://www.tessonics.com/products-riwa.html

[34] Tessonics Corp. (2007). *Resistance Spot Weld Analyzer Software Manual* Retrieved, October 21, 2018, from http://www.tessonics.com/files/rswa/rswa-soft-en-A4.pdf

[35] Wang, L., Hou, Y., Zhang, H., Zhao, J., Xi, T., Qi, X., & Li, Y. (2016). A new measurement method for the dynamic resistance signal during the resistance spot welding process. *Meas. Sci. Technol. 27 095009, 13 pages*

[36] Wang, X., Meng, G., Li, Y. (2011). Monitoring of resistance spot weld quality using electrode vibration signals. *Meas. Sci. Technol. 22 045705, 11 pages*

[37] Zhang, Y., Xuan, C., Wu, P., Su, H., & Ma, Y. (2013) Review on Techniques for On-Line Monitoring of Resistance Spot Welding Process. *Inner Mongolia Agricultural University, China, 7 pages*

[38] Zhang, Y, Chen, G., Lin, Z. (2004). Study on Weld Quality Control of Resistance Spot Welding Using a Neuro-Fuzzy Algorithm. *Lecture Notes in Computer Science, Vol. 3215, pp 544-550*

VITA

Place of Birth: Freeport, The Bahamas

Educational Background:

Year	Degree	Institution
2014	B.S. Systems Engineering	UNC Charlotte

Professional Positions Held:

Year	Employer	Title
2018	The Boeing Company	Mechanical Systems Design & Analysis Engineer 3
2017	Toyota Motors North America	Senior Engineer (Body)
2014	Toyota Motors North America	Process Engineer (Body)
2013	Fiat Chrysler Automobiles	Stamping Manufacturing Intern
2012	Toyota Motors North America	Stamping Co-Op

Ivan Charles Butler

Signature